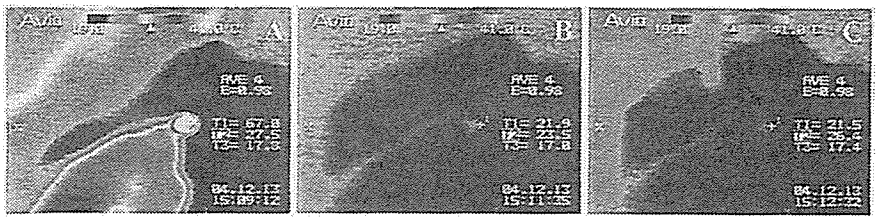

Fig. 2 Thermographic study during simulated endoscope-controlled procedure for intrameatal tumor: the local temperature dramatically increased during drilling of the posterior wall of the IAC (**A**), but normalized thereafter (**B**), and did not changed significantly during the use of endoscope (**C**).

All procedures were planned as routine microneurosurgical operations, so if necessary these could be completed without the use of endoscope. General anesthesia, lateral oblique position of the patient, standard retrosigmoid approach, motor and somatosensory evoked potentials, auditory brain response, facial nerve monitoring, and cochlear nerve action potentials were used routinely, in the same way as described elsewhere [13,14,19,20]. After microsurgical intracapsular debulking of the tumor in the CPA, the posterior wall of the IAC was removed by a high-speed drill. A rigid endoscope fixed in the "EndoArm" was inserted into the CPA under control through an operating microscope. Subsequent removal of the residual tumor from the CPA and IAC was attained utilizing concurrently both microscope- and endoscope-controlled techniques with the use of routine microneurosurgical instruments. Regular irrigation of the wound by Ringer's lactate solution was done during use of the endoscope.

## Results

### Laboratory investigation

The endoscopes with 0°, 30°, and 70° angles of view were found to be equally useful for observation of the CPA through the retrosigmoid approach. Inspection of the IAC seemed to be optimal using the endoscope with a 70° angle of view and outer diameter 4 mm. The insertion of this device into the CPA and its positioning for visualization of the IAC were found to be difficult without microscopic control. Both freehand fixation of the endoscope and use of the "EndoArm" seemed to be equally suitable for inspection of the CPA and IAC. However, endoscope-controlled microsurgical manipulations could not be effectively done without use of the endoscope-holder system, which provided a stable position of the device and allowed bimanual manipulations by the surgeon. During drilling of the posterior wall of the IAC a thermographic study revealed a prominent increase of the local temperature. Alternatively, the presence of an endoscope connected with a working cold light source in the CPA did not lead to significant changes of the local temperature (Fig. **2**).

### Clinical study

Use of the endoscope permitted removal of residual tumor from the most lateral part of the IAC (Fig. **3**). In all, total tumor removal was done in 28 cases, subtotal removal in 3, and partial removal in 2 cases. Anatomic preservation of the facial nerve was attained in 31 cases. In one case the facial nerve was mechanically damaged by the endoscope itself, which necessitated its direct suturing in the CPA. In 8 out of 16 patients, who showed serviceable hearing preoperatively, this was preserved after tumor removal. No one case of thermal injury to the cranial nerves, postoperative CSF leak, or infection was observed. Histological examination revealed typical schwannomas in all cases; mean MIB-1 index constituted 2.3 ± 1.9%.

Final endoscopic inspection at the end of the procedure gives us an opportunity to define the nerve of tumor origin, either definitely (in 18 cases), or most probably (in 14 cases). Schwannomas arising from the superior vestibular and inferior vestibular nerves were represented in 16 cases each (Figs. **4** and **5**). In one case with partial tumor removal the nerve of tumor origin was not defined. Its identification was found to be easier if dilatation of the fundus of the IAC due to tumor growth was present. Meanwhile, no associations were found between the nerve of tumor origin and age and gender of the patient, side and MIB-1 index of the neoplasm, and the presence of useful hearing before surgery.

### Discussion

Modern neuroendoscopic devices, both rigid and flexible, provide a wide angle of view, superb illumination with a cold light, and perfect depth of focus in combination with high magnification. Their use during microsurgical procedures allows to reduce the size of the craniotomy, to improve visualization in the operative field, and to look around important anatomic structures, thus eliminating the need for extensive retraction [4,6,11–13,21–23]. Furthermore, the development of "virtual endoscopy" [24,25], which permits to simulate the surgical procedures preoperatively, based on the data of neuroimaging, can significantly increase the clinical efficacy of the technique in the future.

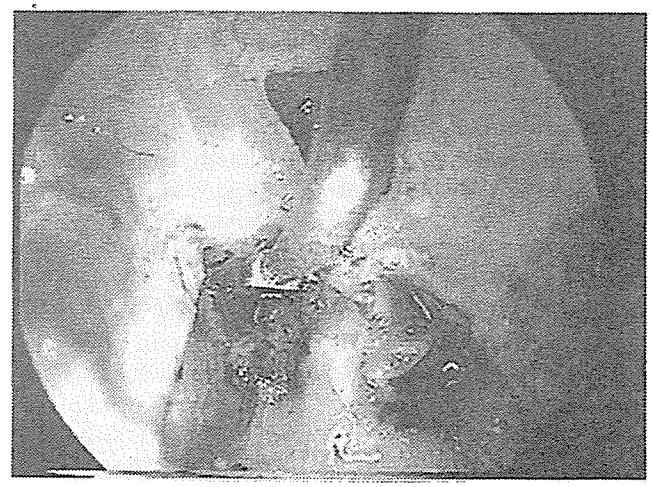

Fig. 3 Endoscope-controlled removal of the intrameatal vestibular schwannoma from the lateral part of the IAC.

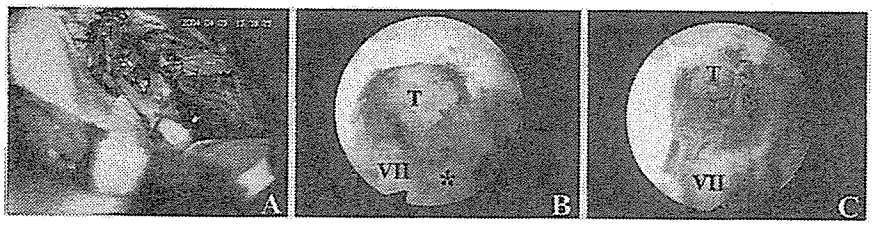


Fig. 4 Endoscope-controlled microneurosurgical removal of the right-sided vestibular schwannoma: view of the tumor in the IAC after removal of its posterior wall (**A**) and observation of the neoplasm originated from the superior vestibular nerve in the most lateral part of IAC (**B** and **C**). Marked: facial nerve (VII), cochlear nerve (asterisk), and tumor (T).

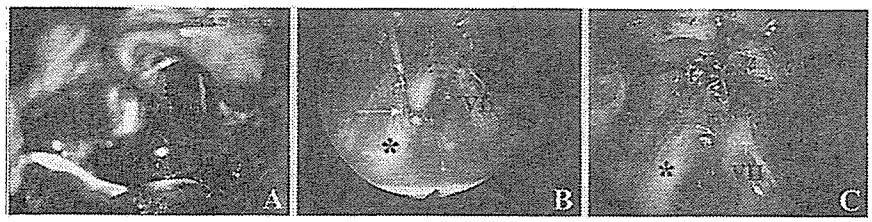


Fig. 5 Endoscope-controlled microneurosurgical removal of the left-sided vestibular schwannoma: view of the tumor after removal of the posterior wall of the IAC (**A**) and endoscopic observation of the neoplasm originated from the inferior vestibular nerve in the most lateral part of the IAC (**B** and **C**). Marked: facial nerve (VII), cochlear nerve (asterisk), tumor (*T*), and electrode for cochlear nerve action potentials (white arrow).





The advantages of the endoscopic inspection during microsurgical removal of vestibular schwannomas had been highlighted in several previous reports [3–15]. These mainly include early identification of the cranial nerves in the CPA, possibility of revision of the most lateral part of the IAC for the presence of the residual neoplasm, and visualization of the non-sealed petrous bone air cells for prevention of postoperative CSF leak. With the adjunct of endoscopy, tumors can be removed more completely, with less morbidity, and the degree of their resection can be assessed more precisely [3,7,10,13,23]. The length of drilling of the posterior wall of the IAC can be reduced, and inadvertent opening of the intraosseous endolymphatic sac and posterior semicircular canal, which has a crucial importance in hearing-preservation vestibular schwannoma surgery, can be avoided [9–12]. The technique may be useful for identification of the source of problematic bleeding during removal of the neoplasm [15]. Finally, as was shown in the present series, use of the endoscope permits an exact delineation of the nerve of tumor origin.

While endoscopic inspection during surgery for vestibular schwannomas has obtained widespread acceptance, the advantages of endoscope-controlled removal of these tumors are less clear. Wackym et al. [13] and Magnan et al. [14] advocated use of this technique for the dissection of the residual neoplasm from the most lateral part of the IAC. Goksu et al. [10] reported the results of such procedures in 8 patients with serviceable hearing and small intrameatal vestibular schwannomas: total removal, functional preservation of the facial nerve, and anatomic preservation of the cochlear nerve was attained in all cases, whereas useful hearing was preserved in four cases. In the present series, which included a significant proportion of large tumors, total removal of the neoplasm was attained in 85% of the cases, anatomic preservation of the facial nerve in 94% of cases, and preservation of the serviceable hearing in 50% of those, who showed its presence before surgery.

Our clinical results confirm that integration of endoscope-controlled removal of the intrameatal part of the tumor into microneurosurgical excision of vestibular schwannomas is technically feasible, effective, and safe. Nevertheless, several lessons have been learnt. First, use of rigid endoscopes, which are usually recommended for endoscope-assisted skull base surgery [6,21,23], may be complicated during endoscope-controlled procedures due to nearly coaxial positions of the endoscopic device and microinstruments. This disadvantage can be overcome if bayonet-style endoscopes and microinstruments are used. Second, several endoscopes should be available during surgery and used according to the particular goals. While 0°, 30°, and 70° angles of view endoscopes were found to be useful for manipulations in the CPA, only the latter device was suitable for observation of the IAC. Third, angled rigid endoscopes may be difficult to pass in the operative wound without risk of inadvertent damage to the neurovascular structures [5,6,23]. Mechanical injury of the facial nerve by the endoscope was met once in the present series. Therefore, we strongly recommend microscopic guidance during insertion of the 70° angle of view device into the CPA.

There is known concern that prolonged use of endoscope can be accompanied by an increase of the local temperature in the vicinity to its tip followed by thermal injury to critical neurovascular structures [11,13]. This was not, however, confirmed by the conducted laboratory thermographic study. In fact, it was found that local temperature in the CPA during the use of an endoscope connected with a working light source, is much lower, compared with those during removal of the posterior wall of the IAC by a high-speed drill. Moreover, in no one case of our clinical series the thermal injury to the cranial nerves was marked. Definitely, the possibility of this complication may depend on the model of the device, duration of its use, type of light source, and individual sensitivity of the cranial nerves. However, in general, the risk of thermal injury during use of the endoscope should not be considered too high, and regular irrigation of the wound by Ringer's lactate solution seems to serve as a sufficient preventive measure.

Intracranial neuroendoscopic procedures are usually performed through a narrow corridor in the vicinity to important neurovascular structures. While endoscopic inspection can be done by

freehand fixation of the device, endoscope-controlled microneurosurgical manipulations require its precise position, because monomanual surgical manipulations may be not only non-effective, but even dangerous if an occasional shift of the endoscope occurs in the surgical wound [5,9–11,13,21–23]. This necessitates the use of special holder, which can provide a stable position of the device in the surgical wound and permits bimanual manipulations by the surgeon and assistant. Several such systems are currently available. One of these is the "EndoArm", which was used in the present study, and can be suitable for endoscopic inspection, endoscope-assisted, and endoscope-controlled microneurosurgery. It provides excellent maneuverability within 6 degrees of freedom, smooth manipulations with avoidance of strenuous maneuvers of the surgeon, accurate fixation in any direction, and safe release, which result in a high level of clinical safety of the device [16].

## Conclusion

Endoscopic inspection during surgery for vestibular schwannomas allows early identification of the cranial nerves, revision of the most lateral part of the IAC for presence of the residual neoplasm, delineation of the nerve of its origin, and visualization of the non-sealed petrous bone air cells for prevention of postoperative CSF leak. Endoscope-controlled microneurosurgical removal of the intrameatal tumors is technically feasible, effective, and safe, and permits to attain dissection of the neoplasm from the most lateral part of the IAC. The risk of thermal injury to the cranial nerves due to use of endoscopes seems to be low. Nevertheless, special training is absolutely necessary, because endoscopic procedures are accompanied by definite learning curve. Availability of good equipment, including an endoscope-holder system, is also very important for attainment of optimal surgical results.

## References


[1] Chernov M, DeMonte F. Skull base tumors. In: Levin VA (ed). Cancer in the nervous system, 2nd edn. Oxford: Oxford University Press, 2002: 300–319

[2] Yamakami I, Uchino Y, Kobayashi E, Yamaura A. Conservative management, gamma-knife radiosurgery, and microsurgery for acoustic neurinomas: a systematic review of outcome and risk of three therapeutic options. Neurol Res 2003; 25: 682–690

[3] McKennan KX. Endoscopy of the internal auditory canal during hearing conservation acoustic tumor surgery. Am J Otol 1993; 14: 259–262

[4] Magnan J, Chays A, Lepetre C, Pencroffi E, Locatelli P. Surgical perspectives of endoscopy of the cerebellopontine angle. Am J Otol 1994; 15: 366–370

[5] Rosenberg SI, Silverstein H, Willcox TO, Gordon MA. Endoscopy in otology and neurootology. Am J Otol 1994; 15: 168–172

[6] Matula C, Tschabitscher M, Diaz Day J, Reinprecht A, Koos WT. Endoscopically assisted microneurosurgery. Acta Neurochir (Wien) 1995; 134: 190–195

[7] Tatagiba M, Matthies C, Samii M. Microendoscopy of the internal auditory canal in vestibular schwannoma surgery: technique application. Neurosurgery 1996; 38: 737–740

[8] Valtonen HJ, Poe DS, Heilman CB, Tarlov EC. Endoscopically assisted prevention of cerebrospinal fluid leak in suboccipital acoustic neuroma surgery. Am J Otol 1997; 18: 381–385

[9] Jennings CR, O'Donoghue GM. Posterior fossa endoscopy. J Laryngol Otol 1998; 112: 227–229

[10] Goksu N, Bayazit Y, Kemaloglu Y. Endoscopy of the posterior fossa and dissection of acoustic neuroma. J Neurosurg 1999; 91: 776–780

[11] King WA, Wackym PA. Endoscope-assisted surgery for acoustic neuromas (vestibular schwannomas): early experience using the rigid Hopkins telescope. Neurosurgery 1999; 44: 1095–1102

[12] Low WK. Enhancing hearing preservation in endoscopic-assisted excision of acoustic neuroma via the retrosigmoid approach. J Laryngol Otol 1999; 113: 973–977

[13] Wackym PA, King WA, Poe DS, Meyer GA, Ojemann RG, Barker FG, Walsh PR, Staecker H. Adjunctive use of endoscopy during acoustic neuroma surgery. Laryngoscope 1999; 109: 1193–1201

[14] Magnan J, Barbieri M, Mora R, Murphy S, Meller R, Bruzzo M, Chays A. Retrosigmoid approach for small and medium-sized acoustic neuromas. Otol Neurotol 2002; 23: 141–145

[15] Gerganov VM, Romansky KV, Bussarsky VA, Noutchev LT, Iliev IN. Endoscope-assisted microsurgery of large vestibular schwannomas. Minim Invas Neurosurg 2005; 48: 39–43

[16] Morita A, Okada Y, Kitano M, Hori T, Taneda M, Kirino T. Development of hybrid integrated endoscope-holder system for endoscopic microneurosurgery. Neurosurgery 2004; 55: 926–932

[17] House WF, Brackmann DE. Facial nerve grading system. Otolaryngol Head Neck Surg 1985; 93: 184–193

[18] Gardner G, Robertson JH. Hearing preservation in unilateral acoustic neuroma surgery. Ann Otol Rhinol Laryngol 1988; 97: 55–66

[19] Ojemann RG. Retrosigmoid approach to acoustic neuroma (vestibular schwannoma). Neurosurgery 2001; 48: 553–558

[20] Ciric I, Zhao J-C, Rosenblatt S, Wiet R, O'Shaughnessy B. Suboccipital retrosigmoid approach for removal of vestibular schwannomas: facial nerve function and hearing preservation. Neurosurgery 2005; 56: 560–570

[21] Perneczky A, Fries G. Endoscope-assisted brain surgery: Part 1 – evolution, basic concept, and current technique. Neurosurgery 1998; 42: 219–225

[22] Fries G, Perneczky A. Endoscope-assisted brain surgery: Part 2 – analysis of 380 procedures. Neurosurgery 1998; 42: 226–232

[23] Teo C. Endoscopic-assisted tumor and neurovascular procedures. Clin Neurosurg 2000; 46: 515–525

[24] Boor S, Maurer J, Mann W, Stoeter P. Virtual endoscopy of the inner ear and the auditory canal. Neuroradiology 2000; 42: 543–547

[25] Vrabec JT, Briggs RD, Rodriguez SC, Johnson Jr RF. Evaluation of the internal auditory canal with virtual endoscopy. Otolaryngol Head Neck Surg 2002; 127: 145–152

# Cerebral Oxygen Metabolism and Neuronal Integrity in Patients With Impaired Vasoreactivity Attributable to Occlusive Carotid Artery Disease

Satoshi Kuroda, MD, PhD; Tohru Shiga, MD, PhD; Kiyohiro Houkin, MD, PhD;
Tatsuya Ishikawa, MD, PhD; Chietsugu Katoh, MD, PhD;
Nagara Tamaki, MD, PhD; Yoshinobu Iwasaki, MD, PhD

***Background and Purpose***—It is still unclear that impaired cerebrovascular reactivity (CVR) to acetazolamide is comparable to elevated oxygen extraction fraction (OEF) on positron emission tomography (PET) in patients with occlusive carotid diseases. Therefore, in this study, the authors aimed to clarify whether OEF is elevated in all patients with reduced cerebral blood flow (CBF) and CVR (type 3) on single photon emission computed tomography (SPECT), and, if not, to specify the underlying pathophysiology of type 3 but normal OEF.

***Methods***—This study included 46 patients who had decreased CBF and CVR on *N*-isopropyl-*p*-$^{123}$I-iodoamphetamine SPECT in the ipsilateral middle cerebral artery area attributable to occlusive carotid diseases. Hemodynamic and metabolism parameters were determined in all patients by $^{15}$O-gas PET, and neuronal integrity was evaluated in 19 patients using $^{11}$C-flumazenil (FMZ) PET.

***Results***—OEF was significantly elevated in 20 (43.5%) of 46 type 3 patients. Another 26 type 3 patients had normal OEF. Regression analysis showed that OEF significantly correlated with cerebral metabolic rate for oxygen and $^{11}$C-FMZ binding potential but not with other parameters. Subcortical infarction had no significant effect on OEF values.

***Conclusions***—The results strongly suggest that type 3 patients with reduced CBF and CVR may be divided into 2 pathophysiologically different subgroups: misery perfusion attributable to hemodynamic compromise and matched hypometabolism attributable to incomplete infarction. Type 3 but normal OEF may represent a transition stage from misery perfusion to matched hypometabolism. (***Stroke.*** **2006;37:393-398.)**

**Key Words:** acetazolamide ■ cerebral ischemia ■ flumazenil ■ metabolism ■ oxygen

There is increasing evidence that hemodynamically compromised patients with internal carotid artery (ICA) occlusion are at higher risk for subsequent ischemic stroke. Over these 20 years, an elevated oxygen extraction fraction (OEF) determined by positron emission tomography (PET) has been believed to represent critical reduction of cerebral perfusion pressure, named as "misery perfusion" or "stage II."[1,2] Recent statistical analyses have proven that an elevated OEF can be an independent risk factor for subsequent ischemic stroke in patients with occlusive carotid artery disease.[3–5]

Alternatively, cerebrovascular reactivity (CVR) to $CO_2$ or acetazolamide has also been used to assess cerebral perfusion reserve in patients with occlusive carotid diseases because single photon emission computed tomography (SPECT) or cold xenon computed tomography (CT) is more widely available and can be done at lower costs than PET. Recent studies have proven that quantitative measurements of cerebral blood flow (CBF) and CVR can also be a predictor for subsequent ischemic stroke in patients with ICA or middle cerebral artery (MCA) occlusion. Thus, Kuroda et al (2001) reported that relative risk conferred by reduced CBF and CVR (type 3) was 8.0 (95% CI, 1.9 to 34.4) for ipsilateral stroke.[6] Subsequently, Ogasawara et al also reported similar results.[7] Based on these observations, SPECT has been expected to identify misery perfusion or stage II more easily than PET if CVR is comparable to OEF.[8]

However, it is still controversial whether impaired CVR is directly linked to OEF elevation in patients with occlusive carotid artery diseases or not. Thus, previous studies have reported a significant correlation between OEF and CVR to acetazolamide or $CO_2$.[9–14] However, the number of patients included in these studies was not so large, and their hemodynamic and metabolic parameters varied widely among the subjects. On the other hand, recent study has shown that ≈40% of patients with reduced CVR have normal OEF when both parameters are evaluated in each patient.[15] The issue is

Received September 29, 2005; final revision received November 8, 2005; accepted November 13, 2005.

From the Departments of Neurosurgery (S.K., T.I., Y.I.) and Nuclear Medicine (T.S., C.K., N.T.), Hokkaido University Graduate School of Medicine, Japan; and Department of Neurosurgery (K.H.), Sapporo Medical University, Japan.

Correspondence to Satoshi Kuroda, MD, PhD, Department of Neurosurgery, Hokkaido University Graduate School of Medicine, North 15 West 7, Kita-ku, Sapporo 060-8638, Japan. E-mail skuroda@med.hokudai.ac.jp



*Stroke* **is available at http://www.strokeaha.org** **DOI: 10.1161/01.STR.0000198878.66000.4e**

quite important because there may be a significant difference in sensitivity for detecting the patients at higher risk for subsequent stroke between CVR and OEF.

On the other hand, $^{11}$C-flumazenil (FMZ) PET has been accepted as a noninvasive, variable tool to investigate neuronal integrity because FMZ is a specific ligand to the central type of benzodiazepine receptors that are exclusively localized in the neurons. Recent studies have shown that $^{11}$C-FMZ PET can detect ischemia-induced selective neuronal necrosis that is not visible on either CT or MRI.[16,17]

Therefore, in this study, the authors aimed to clarify whether OEF is elevated in all patients who are diagnosed as type 3 on SPECT, and, if not, to specify the underlying pathophysiology of normal OEF in spite of type 3. For this purpose, the authors measured the parameters for oxygen metabolism and for neuronal integrity in type 3 patients with occlusive, using $^{15}$O-gas and $^{11}$C-FMZ PET, respectively.

## Subjects and Methods

### Patients

The present study included a total of 46 patients who were admitted to our hospital between January 1999 and December 2004. All of them met the following criteria: (1) severe stenosis (>90%) or occlusion of the ipsilateral ICA or MCA; (2) no or, if any, small infarction on MRI; and (3) reduced CBF and CVR to acetazolamide in the ipsilateral MCA territory on [$^{123}$I]*N*-isopropyl-*p*-iodoamphetamine ($^{123}$I-IMP) SPECT (see below). There were 36 men and 10 women with a mean age of 68.2 years (range 48 to 79 years). Their clinical symptoms included transient ischemic attack or amaurosis fugax in 18 patients and minor completed stroke (Rankin score 1 or 2) in 25. The other 3 patients were asymptomatic. Digital subtraction angiography showed ICA occlusion in 27 patients, ICA severe stenosis in 8, MCA occlusion in 5, and MCA severe stenosis in 6. All studies were performed ≥4 weeks after the last ischemic episode because the studies in an earlier period might affect the correct interpretation of the data.[18]

### SPECT Measurements

All patients were scanned with a triple-head γ camera (GCA-9300/DI; Toshiba) to determine CBF and CVR to acetazolamide, as described previously.[16] Briefly, quantitative blood flow was determined by using the $^{123}$I-IMP injection and single-scan autoradiographic technique. CBF was quantitatively measured before and 15 minutes after intravenous injection of 10 mg/kg acetazolamide on the separate days with an interval of 2 to 3 days. To evaluate cerebral hemodynamics, 10-mm diameter circular regions of interest (ROIs) were symmetrically placed in the ipsilateral and contralateral MCA territories. As described previously,[6,18,19] CVR to acetazolamide was quantitatively calculated as: CVR (%)=100×($CBF_{ACZ}$−$CBF_{rest}$)/$CBF_{rest}$, where $CBF_{rest}$ and $CBF_{ACZ}$ represent CBF before and after intravenous injection of acetazolamide, respectively. Normal control values of CBF (mean±SD=38.1±5.4 mL/min per 100 g) and CVR (30.0±8.0%) in the MCA territory were obtained from 10 normal volunteers free of cerebrovascular disease. The values were rated as reduced when any of them were less than mean−2 SD. Thus, in the current study, patients were judged as type 3 when CBF was <27 mL/min per 100 g and CVR was <14%.[16]

### PET Measurements

All patients were scanned with ECAT EXACT HR+ (Siemens) as described previously.[16] The intervals between SPECT and PET measurements were within 2 weeks. One-minute inhalation of $^{15}$O-CO (2 GBq/min) followed by 3-minute static scanning and 3-time arterial blood sampling were performed to measure cerebral blood volume (CBV). After 15-minute inhalation of $^{15}$O-$O_2$ (0.5 GBq/min), a steady-state $O_2$ image was scanned and 3-time arterial blood sampling was performed for 5 minutes to measure OEF and cerebral metabolic rate for oxygen ($CMRO_2$). Finally, to determine CBF, steady-state $CO_2$ image was scanned and 3-time arterial blood sampling was performed for 5 minutes after 15-minute inhalation of $^{15}$O-$CO_2$ (0.5 GBq/min). Normal PET values were obtained from 10 volunteers: CBF, 44±4 mL/min per 100 g; $CMRO_2$, 3.3±0.6 mL/min per 100 g; CBV, 3.7±0.7 mL/min, and OEF, 0.43±0.05 (mean±SD). Each PET parameter was obtained using 10-mm diameter circular ROIs. The values were rated as decreased when any of them were less than mean−2 SD and rated as increased when any of them were more than mean+2 SD.

The dynamic FMZ PET was studied in 19 of 46 patients at the same time that $^{15}$O-gas PET was performed, as reported previously.[16] Briefly, the injected dose of $^{11}$C-FMZ was 370 MBq for each patient. The binding potential (BP) images were calculated pixel by pixel using the reference tissue model.[20]

### Data Analysis

To evaluate various parameters obtained from $^{123}$I-IMP SPECT, $^{15}$O-gas PET, and $^{11}$C-FMZ PET, the SPECT and PET images were automatically coregistered to axial T1-weighted MRI images. The SPECT, PET, and MRI images were registered using fully automatic multimodality image registration algorithm on Unix-based workstation (Indigo 2; SGI Inc.).[21]

All data were expressed as mean±SD. The data between 2 groups were compared by use of $\chi^2$ test or paired *t* test as appropriate. Differences with a *P* value of <0.05 were considered statistically significant.

## Results

### $^{15}$O PET Parameters

CBF, CBV, $CMRO_2$, and OEF in type 3 patients are shown in the Table. There were significant differences in CBF, $CMRO_2$, and OEF between the ipsilateral and contralateral MCA areas. However, there was no significant difference in CBV between them.

Relationships between OEF and other PET parameters were analyzed in the ipsilateral hemispheres (Figure 1). There was no significant correlation between OEF and CBF ($R^2$=0.001;

**Quantitative Data of Hemodynamic and Metabolic Parameters in the Ipsilateral and Contralateral MCA Areas in Type 3 Patients**

| | Type 3 Patients | | | |
|---|---|---|---|---|
| | Ipsilateral MCA Area | Contralateral MCA Area | Significance | Control Value |
| n | 46 | 46 | | 10 |
| CBF, mL/100 g/min | 24.8±4.5 | 31.9±6.3 | *P*<0.0001 | 44.0±4.0 |
| CBV, mL/100 g | 4.2±1.1 | 3.8±1.1 | NS | 3.70±0.70 |
| $CMRO_2$, mL/100 g/min | 1.98±0.48 | 2.27±0.48 | *P*=0.0045 | 3.30±0.60 |
| OEF | 0.46±0.09 | 0.40±0.05 | *P*<0.0001 | 0.43±0.05 |

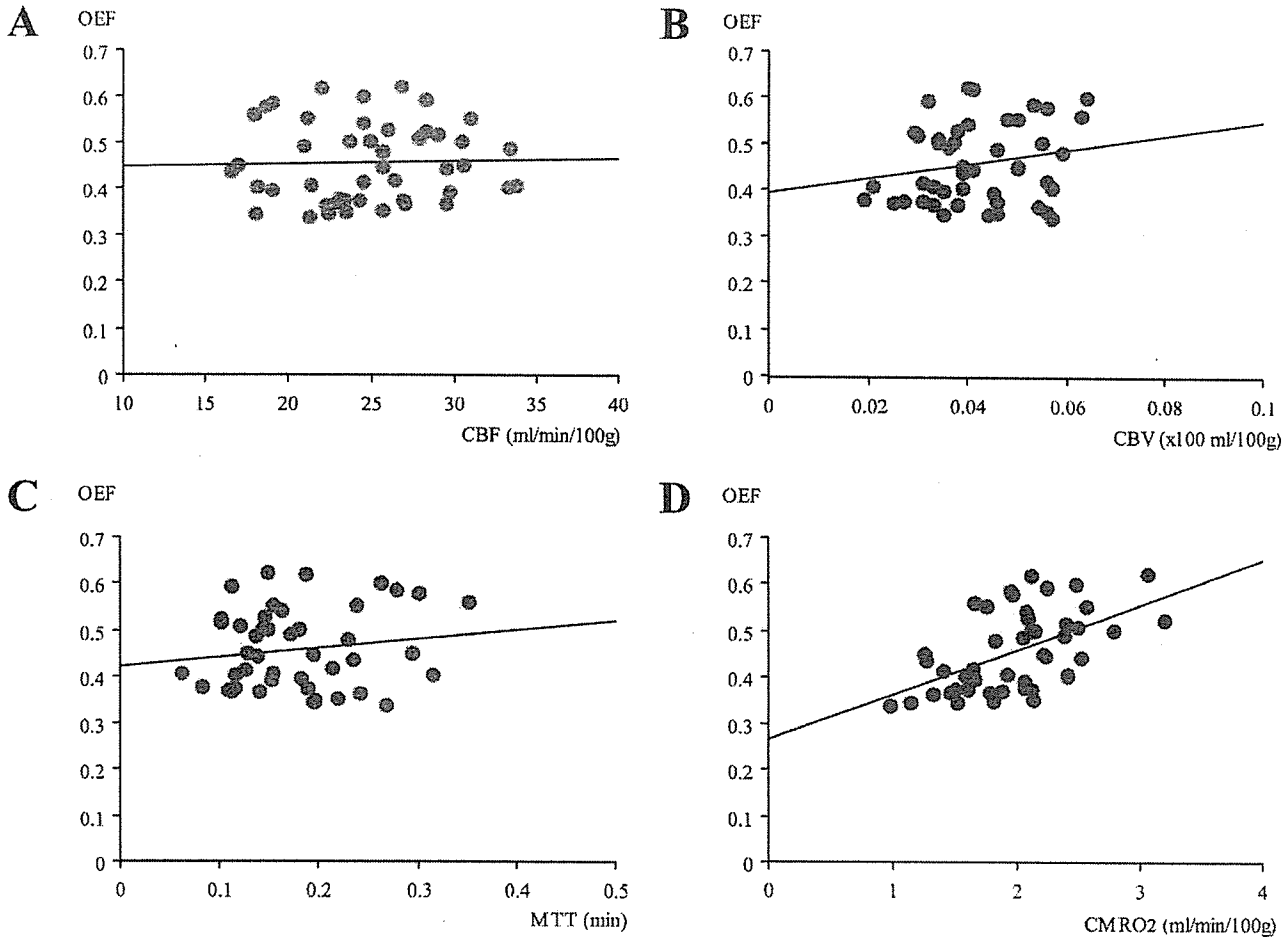


**Figure 1.** Regression analysis of the relationships between OEF and CBF (A), CBV (B), MTT (C), or $CMRO_2$ (D) in 46 type 3 patients.

$P$=0.841), between OEF and CBV ($R^2$=0.041; $P$=0.1794), or between OEF and mean transit time (MTT; $R^2$=0.023; $P$=0.3169). On the other hand, there was significant, positive correlation between OEF and $CMRO_2$ ($R^2$=0.081; $P$=0.006).

Then the values of OEF, $CMRO_2$, and CBV were evaluated in each patient. Although OEF was significantly higher in the ipsilateral MCA area than in the contralateral side, OEF was significantly elevated in only 20 (43.5%) of 46 patients. OEF was kept within normal limits in the other 26 patients (Figure 2).

$CMRO_2$ was significantly higher in patients with elevated OEF than in those with normal OEF: 2.26±0.41 and 1.78±0.42 mL/100 g per minute, respectively ($P$=0.0002; Figure 3). Of 20 patients with elevated OEF, 14 (70%) had normal $CMRO_2$ and the other 6 (30%) had decreased $CMRO_2$ (<2.1 mL/100 g per minute). On the other hand, of 26 patients with normal OEF, 7 (26.9%) had normal $CMRO_2$ and the other 19 (73.1%) had decreased $CMRO_2$. Thus, normal $CMRO_2$ was more frequently observed in patients with elevated OEF than in those with normal OEF ($P$=0.0032; Figure 3).

There was no significant difference in CBV between patients with elevated OEF and with normal OEF: 4.4±1.1 and 4.0±1.1 mL/100 g, respectively ($P$=0.2357; Figure 3). However, of 20 patients with elevated OEF, 9 (45%) had increased CBV. Of 26 patients with normal OEF, only 4 (15.4%) had increased CBV. As the result, increased CBV was more frequently denoted in patients with elevated OEF than in those with normal OEF ($P$=0.0264; Figure 3).

### $^{11}$C-FMZ Binding Potential

To evaluate the neuronal integrity in patients with type 3 ischemia, $^{11}$C-FMZ PET was performed in 19 (41.3%) of 46 patients. The relationships between the ratio of the ipsilateral to contralateral $^{11}$C-FMZ BP and metabolic parameters were analyzed. There was a significant, positive correlation between the ratio and OEF ($R^2$=0.507; $P$=0.0006; Figure 4). The ratio also significantly correlated with $CMRO_2$ ($R^2$=0.324; $P$=0.011).

### MRI

Using T2-weighted MRI, the localization of cerebral infarction was evaluated to clarify its effects on cerebral oxygen metabolism and neuronal integrity. Subcortical infarction in the ipsilateral hemisphere was found in 7 of 20 patients with elevated OEF and in 16 of 26 patients with normal OEF. There was no significant effect of subcortical infarction on OEF value in type 3 patients ($\chi^2$ test $P$=0.0743).

## Discussion

The present results revealed that hemodynamic and metabolic parameters in type 3 patients are not uniform, and that they

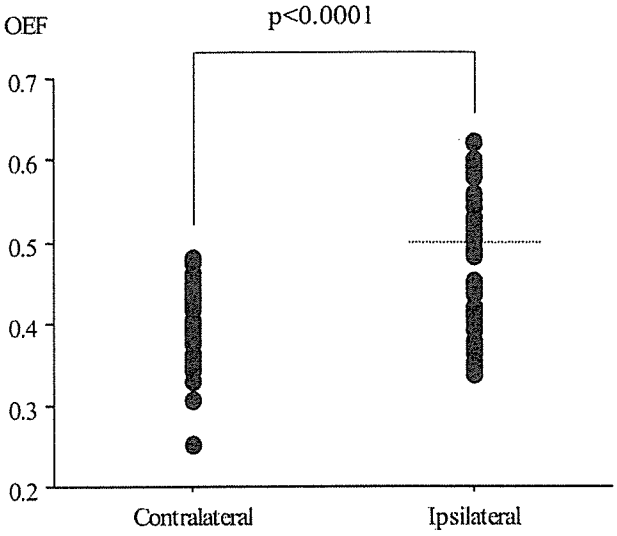


**Figure 2.** Plot of OEF values in the ipsilateral and contralateral hemisphere of type 3 patients. Dotted line indicates the upper limit of normal OEF value.

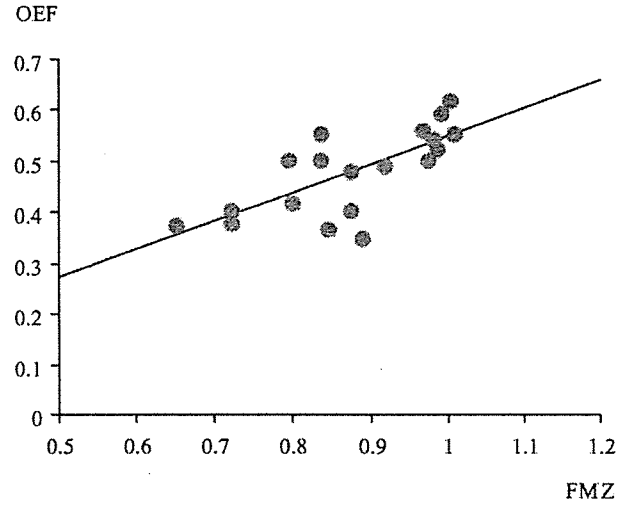


**Figure 4.** Regression analysis of the relationship between OEF and the BP for $^{11}$C-FMZ in 19 type 3 patients.

can be largely classified into 2 subgroups according to OEF value. OEF was significantly elevated in ≈40% of type 3 patients and was within normal limits in the others, indicating that type 3 is not always identical to misery perfusion or stage II. $CMRO_2$ was significantly higher in patients with elevated OEF than in those with normal OEF (Figure 3A) and significantly correlated with OEF (Figure 1D). Therefore, OEF may depend on the metabolic demand in the ischemic tissue.

As the next step, $^{11}$C-FMZ BP and the localization of cerebral infarction were evaluated to specify the underlying pathophysiology of $CMRO_2$ reduction in the area with type 3 but normal OEF. Subcortical infarction in the ipsilateral hemisphere was not directly related to type 3 but normal OEF, although previous reports suggested its involvement.[15] However, there was a significant correlation between OEF and the $^{11}$C-FMZ BP in type 3 patients. Because γ-aminobutyric acid receptors are abundant in the cortex and sensitive to ischemic damage, the specific ligand to their subunits, the central type of benzodiazepine receptors, has been used as a marker of preserved morphological integrity. Garcia et al emphasized the importance of selective neuronal necrosis (incomplete infarction) in human stroke as a pathologic entity.[17] Recently, the authors demonstrated that $CMRO_2$ and $^{11}$C-FMZ BP were reduced to ≈80% of the contralateral side, but there was no significant side-to-side difference in CBV and OEF in patients with reduced CBF and normal CVR (type 4) and concluded that type 4 represents oxygen hypometabolism attributable to ischemia-related selective neuronal damage.[16] Previous studies have shown that the patients with type 4 may not be at high risk for subsequent stroke when medically treated.[6,18] The PET parameters in patients with type 3 ischemia but normal OEF are quite similar to those in the patients with type 4.

Based on these observations, type 3 may include 2 pathophysiologically different conditions: misery perfusion (or stage II ischemia) attributable to hemodynamic compromise, and matched hypometabolism attributable to incomplete infarction. Although the authors have simply graded cerebral hemodynamics of the patients with occlusive carotid artery diseases into 4 types, type 3 should be subdivided into "true type 3," with elevated OEF, and "type 3.5," with normal OEF, in discussing their pathophysiology and long-term prognosis. It is obscure why CVR is impaired in patients with type 3 but normal OEF. As Yamauchi et al pointed out, such

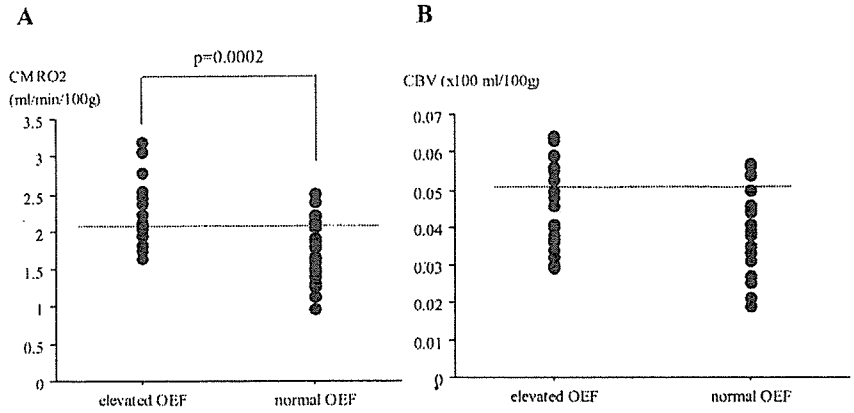


**Figure 3.** Plots of ipsilateral values of $CMRO_2$ (A) and CBV (B) in patients with elevated and normal OEF. Dotted lines indicate the lower limit of normal $CMRO_2$ value (A) and the upper limit of normal CBV value (B).

patients may have complex hemodynamic and metabolic changes in response to both reduced perfusion pressure and ischemic tissue damage.[14]

Present results mirror previous descriptions, that is, using $^{133}$xenon inhalation method and SPECT, the authors divided 32 patients with ICA occlusion into 4 types and serially measured CBF and CVR after superficial temporal artery to MCA anastomosis. Seven patients were diagnosed as having type 3 before surgery. The CVR normalized in all type 3 patients, suggesting postoperative improvement of cerebral perfusion reserve. But CBF returned to normal range in 3 (42.8%) of 7 type 3 patients. As the result, SPECT parameters altered from type 3 to type 4 in other 4 patients.[18] Furthermore, they recently assessed long-term prognosis of 77 patients who were medically treated because of ICA or MCA occlusion. Of 11 type 3 patients, 4 (36.4%) developed ipsilateral ischemic stroke during follow-up periods.[6] The present results may explain these varieties in type 3 patients.

However, as recent studies have clarified, hemodynamic and metabolic responses to reduced perfusion pressure are not so simple. Patients with "classic" misery perfusion (elevated OEF and CBV) are at highest risk for subsequent stroke.[22] However, CBV changes widely vary in patients with occlusive carotid artery disease. This study also showed that CBV widely varied in spite of OEF values. Further studies would clarify the CBV responses to chronic cerebral ischemia more precisely.

This study showed that type 3 is not equal to misery perfusion. However, SPECT and acetazolamide test are still useful modalities because they can simply select the patients at higher risk for subsequent ischemic stroke at lower costs than PET, as described previously.[6,7] Thus, it is very valuable to establish the methodology to detect misery perfusion more efficiently with the use of SPECT because PET is not widely available. Based on a significant linear correlation between OEF and $^{11}$C-FMZ BP in this study, the authors propose to evaluate whether $^{123}$I-iomazenil (IMZ) SPECT can detect misery perfusion or stage II ischemia in type 3 patients more efficiently. $^{123}$I-IMZ is an alternative benzodiazepine receptor ligand for SPECT and has been reported that a reduction of its binding reflects oxidative hypometabolism caused by neuronal damage in hemodynamically impaired areas in patients with cerebrovascular disease.[23–25] Therefore, SPECT may be able to identify the patients with misery perfusion by measuring CVR and $^{123}$I-IMZ binding, if the results on $^{123}$I-IMZ SPECT are comparable to those on $^{11}$C-FMZ PET in patients with occlusive carotid artery diseases.

## Conclusion

Previous studies have shown that type 3 (reduced CBF and CVR) as well as elevated OEF is statistically independent predictors for subsequent stroke in patients with occlusive carotid artery diseases.[3,4,6,26] However, this study clearly showed that OEF was elevated in ≈40% of patients with reduced CBF and CVR (type 3). Significant, positive linear relationships were observed between OEF and $CMRO_2$ and between OEF and $^{11}$C-FMZ BP. Type 3 may include 2 pathophysiologically different conditions: misery perfusion (or stage II) attributable to hemodynamic compromise and matched hypometabolism attributable to incomplete infarction. Further studies would be necessary to define the SPECT parameter to select the patients at higher risk for subsequent stroke more specifically.

## References


1. Baron JC, Bousser MG, Rey A, Guillard A, Comar D, Castaigne P. Reversal of focal "misery-perfusion syndrome" by extra-intracranial arterial bypass in hemodynamic cerebral ischemia. A case study with 15o positron emission tomography. *Stroke*. 1981;12:454–459.
2. Powers WJ, Grubb RL Jr, Raichle ME. Physiological responses to focal cerebral ischemia in humans. *Ann Neurol*. 1984;16:546–552.
3. Grubb RL Jr, Derdeyn CP, Fritsch SM, Carpenter DA, Yundt KD, Videen TO, Spitznagel EL, Powers WJ. Importance of hemodynamic factors in the prognosis of symptomatic carotid occlusion. *J Am Med Assoc*. 1998; 280:1055–1060.
4. Yamauchi H, Fukuyama H, Nagahama Y, Nabatame H, Ueno M, Nishizawa S, Konishi J, Shio H. Significance of increased oxygen extraction fraction in five-year prognosis of major cerebral arterial occlusive diseases. *J Nucl Med*. 1999;40:1992–1998.
5. Derdeyn CP, Videen TO, Grubb RL Jr, Powers WJ. Comparison of pet oxygen extraction fraction methods for the prediction of stroke risk. *J Nucl Med*. 2001;42:1195–1197.
6. Kuroda S, Houkin K, Kamiyama H, Mitsumori K, Iwasaki Y, Abe H. Long-term prognosis of medically treated patients with internal carotid or middle cerebral artery occlusion: can acetazolamide test predict it? *Stroke*. 2001;32:2110–2116.
7. Ogasawara K, Ogawa A, Yoshimoto T. Cerebrovascular reactivity to acetazolamide and outcome in patients with symptomatic internal carotid or middle cerebral artery occlusion: a xenon-133 single-photon emission computed tomography study. *Stroke*. 2002;33:1857–1862.
8. Nemoto EM, Yonas H. Revisiting the question, "is the acetazolamide test valid for quantitative assessment of maximal cerebral autoregulatory vasodilation?" *Stroke*. 2001;32:1234–1237.
9. Kanno I, Uemura K, Higano S, Murakami M, Iida H, Miura S, Shishido F, Inugami A, Sayama I. Oxygen extraction fraction at maximally vasodilated tissue in the ischemic brain estimated from the regional $CO_2$ responsiveness measured by positron emission tomography. *J Cereb Blood Flow Metab*. 1988;8:227–235.
10. Herold S, Brown MM, Frackowiak RS, Mansfield AO, Thomas DJ, Marshall J. Assessment of cerebral haemodynamic reserve: correlation between pet parameters and $CO_2$ reactivity measured by the intravenous 133 xenon injection technique. *J Neurol Neurosurg Psychiatry*. 1988;51: 1045–1050.
11. Hirano T, Minematsu K, Hasegawa Y, Tanaka Y, Hayashida K, Yamaguchi T. Acetazolamide reactivity on $^{123}$I-IMP single photon emission computed tomography in patients with major cerebral artery occlusive disease: correlation with positron emission tomography parameters. *J Cereb Blood Flow Metab*. 1994;14:763–770.
12. Imaizumi M, Kitagawa K, Hashikawa K, Oku N, Teratani T, Takasawa M, Yoshikawa T, Rishu P, Ohtsuki T, Hori M, Matsumoto M, Nishimura T. Detection of misery perfusion with split-dose $^{123}$I-iodoamphetamine single-photon emission computed tomography in patients with carotid occlusive diseases. *Stroke*. 2002;33:2217–2223.
13. Nariai T, Suzuki R, Hirakawa K, Maehara T, Ishii K, Senda M. Vascular reserve in chronic cerebral ischemia measured by the acetazolamide challenge test: comparison with positron emission tomography. *AJNR Am J Neuroradiol*. 1995;16:563–570.
14. Yamauchi H, Okazawa H, Kishibe Y, Sugimoto K, Takahashi M. Oxygen extraction fraction and acetazolamide reactivity in symptomatic carotid artery disease. *J Neurol Neurosurg Psychiatry*. 2004;75:33–37.
15. Nemoto EM, Yonas H, Kuwabara H, Pindzola RR, Sashin D, Meltzer CC, Price JC, Chang Y, Johnson DW. Identification of hemodynamic compromise by cerebrovascular reserve and oxygen extraction fraction in occlusive vascular disease. *J Cereb Blood Flow Metab*. 2004;24: 1081–1089.
16. Kuroda S, Shiga T, Ishikawa T, Houkin K, Narita T, Katoh C, Tamaki N, Iwasaki Y. Reduced blood flow and preserved vasoreactivity characterize oxygen hypometabolism due to incomplete infarction in occlusive carotid artery diseases. *J Nucl Med*. 2004;45:943–949.
17. Garcia JH, Lassen NA, Weiller C, Sperling B, Nakagawara J. Ischemic stroke and incomplete infarction. *Stroke*. 1996;27:761–765.

18. Kuroda S, Kamiyama H, Abe H, Houkin K, Isobe M, Mitsumori K. Acetazolamide test in detecting reduced cerebral perfusion reserve and predicting long-term prognosis in patients with internal carotid artery occlusion. *Neurosurgery*. 1993;32:912–918.
19. Kuroda S, Takigawa S, Kamiyama H, Abe H, Sakuragi M, Motomiya M, Nakagawa T, Mitsumori K, Tsuru M. [diagnosis of hemodynamic compromise in patients with chronic cerebral ischemia: the detection of impaired vasodilatory capacity with 133xe spect and acetazolamide (diamox) test]. *No Shinkei Geka*. 1990;18:167–173.
20. Millet P, Graf C, Buck A, Walder B, Ibanez V. Evaluation of the reference tissue models for pet and spect benzodiazepine binding parameters. *NeuroImage*. 2002;17:928–942.
21. Ardekani BA, Braun M, Hutton BF, Kanno I, Iida H. A fully automatic multimodality image registration algorithm. *J Comput Assist Tomogr*. 1995;19:615–623.
22. Derdeyn CP, Videen TO, Yundt KD, Fritsch SM, Carpenter DA, Grubb RL, Powers WJ. Variability of cerebral blood volume and oxygen extraction: Stages of cerebral hemodynamic impairment revisited. *Brain*. 2002;125:595–607.
23. Hayashida K, Hirose Y, Tanaka Y, Miyashita K, Ishida Y, Miyake Y, Nishimura T. Reduction of $^{123}$I-iomazenil uptake in hemodynamically and metabolically impaired brain areas in patients with cerebrovascular disease. *Nucl Med Commun*. 1996;17:701–705.
24. Makino K, Kamiyama H, Takamura H, Gotoh S, Kobayashi N. Assessment of outcome by ec/ic bypass with $^{123}$I-iomazenil brain spect. *Ann Nucl Med*. 1999;13:261–264.
25. Nakagawara J, Sperling B, Lassen NA. Incomplete brain infarction of reperfused cortex may be quantitated with iomazenil. *Stroke*. 1997;28:124–132.
26. Yamauchi H, Fukuyama H, Nagahama Y, Nabatame H, Nakamura K, Yamamoto Y, Yonekura Y, Konishi J, Kimura J. Evidence of misery perfusion and risk for recurrent stroke in major cerebral arterial occlusive diseases from pet. *J Neurol Neurosurg Psychiatry*. 1996;61:18–25.

**Ken-ichiro Kikuta, M.D., Ph.D.**
Department of Neurosurgery,
Kyoto University
Graduate School of Medicine,
Kyoto, Japan

**Yasushi Takagi, M.D., Ph.D.**
Department of Neurosurgery,
Kyoto University
Graduate School of Medicine,
Kyoto, Japan

**Yasutaka Fushimi, M.D.**
Department of Diagnostic Imaging
and Nuclear Medicine,
Kyoto University
School of Medicine,
Kyoto, Japan

**Kouichi Ishizu, M.D., Ph.D.**
Department of Diagnostic Imaging
and Nuclear Medicine,
Kyoto University
School of Medicine,
Kyoto, Japan

**Tsutomu Okada, M.D.**
Department of Diagnostic Imaging
and Nuclear Medicine,
Kyoto University
Graduate School of Medicine,
Kyoto, Japan

**Takashi Hanakawa, M.D., Ph.D.**
Human Brain Research Center,
Kyoto University
School of Medicine,
Kyoto, Japan

**Yukio Miki, M.D., Ph.D.**
Department of Diagnostic Imaging
and Nuclear Medicine,
Kyoto University
School of Medicine,
Kyoto, Japan

**Hidenao Fukuyama, M.D., Ph.D.**
Human Brain Research Center,
Kyoto University
School of Medicine,
Kyoto, Japan

**Kazuhiko Nozaki, M.D., Ph.D.**
Department of Neurosurgery,
Kyoto University
Graduate School of Medicine,
Kyoto, Japan

**Nobuo Hashimoto, M.D., Ph.D.**
Department of Neurosurgery,
Kyoto University
Graduate School of Medicine,
Kyoto, Japan

**Reprint requests:**
Ken-ichiro Kikuta, M.D., Ph.D.,
Department of Neurosurgery,
Kyoto University
Graduate School of Medicine,
54 Kawaharacho,
Shogoin, Sakyo-ku,
Kyoto 606-8507, Japan.
Email: kikuta@kuhp.kyoto-u.ac.jp

**Received,** December 28, 2005.
**Accepted,** June 1, 2006



# "TARGET BYPASS": A METHOD FOR PREOPERATIVE TARGETING OF A RECIPIENT ARTERY IN SUPERFICIAL TEMPORAL ARTERY-TO-MIDDLE CEREBRAL ARTERY ANASTOMOSES

**OBJECTIVE:** To introduce a method for preoperative targeting of a proper recipient artery in superficial temporal artery-to-middle cerebral artery anastomosis.

**METHODS:** Six operations for superficial temporal artery-to-middle cerebral artery anastomosis in four patients with moyamoya disease or moyamoya-like disease and two operations in two patients with atherosclerotic cerebrovascular occlusive disease accompanied by coronary artery stenosis were performed using our method. Before surgery, a 3-Tesla magnetic resonance imaging study was performed with axial T1-weighted three-dimensional magnetization-prepared rapid acquisition gradient-echo sequences and three-dimensional time-of-flight magnetic resonance angiography. Data on quantitative regional cerebral blood flow were obtained by iodine-123-labeled N-isopropyl-iodoamphetamine single-photon emission computed tomography or positron emission computed tomography. The magnetic resonance angiography and regional cerebral blood flow data sets were registered with the magnetization-prepared rapid acquisition gradient-echo data set by means of the coregistration function of the SPM2 software. We examined the arteries located on or near the cortex where the regional cerebral blood flow had significantly decreased and used the coregistered data set and MRIcro software to select the cortical artery with the largest diameter as the target recipient artery. At the surgery, the data sets were applied to the neuronavigation system and the actual site of the target was confirmed in the operation before scalp incision. The superficial temporal artery was anastomosed with the target through a small craniotomy.

**RESULTS:** Successful bypass surgery to the target was confirmed in all cases.

**CONCLUSION:** The "target bypass" method might be effective for cases with moyamoya disease or for cases requiring surgery through a small craniotomy.

**KEY WORDS:** Cerebral blood flow, Coregistration, Moyamoya disease, Neuronavigation, Recipient, Superficial temporal artery-to-middle cerebral artery anastomosis, Target

*Neurosurgery 59[ONS Suppl 4]:ONS-320–ONS-327, 2006* DOI: 10.1227/01.NEU.0000232775.06672.F4

Superficial temporal artery-to-middle cerebral artery (STA-MCA) anastomosis was first reported by Yaşargil (22) in 1969. In Japan, STA-MCA has especially been applied to the treatment of moyamoya disease (MMD) (8, 13), a progressive steno-occlusive disease at the terminal portion of the bilateral internal carotid arteries (ICAs) with the development of moyamoya vessels as collateral channels (4). Although direct bypass is reported to be more effective than indirect bypass, such as encephaloduroarteriosynangiosis, for improved clinical and radiological treatment of MMD (2, 7, 10, 12, 18), it is often disregarded because of its technical difficulty (11). One reason is the difficulty of finding suitable recipient arteries during the operation because the diameter of most cortical branches of the MCA is small in patients with MMD (9, 10, 13). Recent advances in neuroradiology

TABLE 1. Patient characteristics[a]

| Patient no. | Age (yr)/sex | Disease entity | Side | Procedure | Diameter of craniotomy (mm) |
|---|---|---|---|---|---|
| 1 | 29/M | MMD | Left | STA-MCA | 25 |
| | | | Right | STA-MCA | 20 |
| 2 | 67/F | MMD | Right | STA-MCA + EMS | 40 |
| 3 | 57/F | Moyamoya-like disease underlying diabetes mellitus | Right | STA-MCA | 30 |
| | | | Left | STA-MCA | 20 |
| 4 | 63/F | MMD | Left | STA-MCA | 20 |
| 5 | 73/M | ICA occlusion accompanied with coronary artery stenosis | Left | STA-MCA | 20 |
| 6 | 71/M | MCA occlusion accompanied with coronary artery stenosis | Right | STA-MCA | 20 |

[a] MMD, moyamoya disease; STA-MCA, superficial temporal artery-to-middle cerebral artery; EMS, encephalo-myo-synangiosis; ICA, internal carotid artery.

and image-guided navigation surgery have resulted in the surgical use of fusion images obtained through various kinds of neuroradiological studies (1, 6, 17). Here, we present a method for the preoperative targeting of an appropriate recipient artery in STA-MCA anastomosis and introduce our initial experiences applying our method for cerebrovascular occlusive disease, such as MMD.

## Patient Summary

Six operations for STA-MCA anastomosis in four patients with MMD or moyamoya-like disease and two operations in two patients with atherosclerotic cerebrovascular occlusive disease accompanied with coronary artery stenosis were performed using our method. *Table 1* shows the characteristics of the patients.

## Imaging Study and Data Processing

Before surgery, a magnetic resonance imaging study was performed with a 3-Tesla magnetic resonance scanner (Magnetom Trio; Siemens, Erlargen, Germany) with magnetization-prepared rapid acquisition gradient-echo (MPRAGE) sequences (repetition time [TR], 2000; echo time [TE], 4.4; time interval [TI], 990 ms; flip

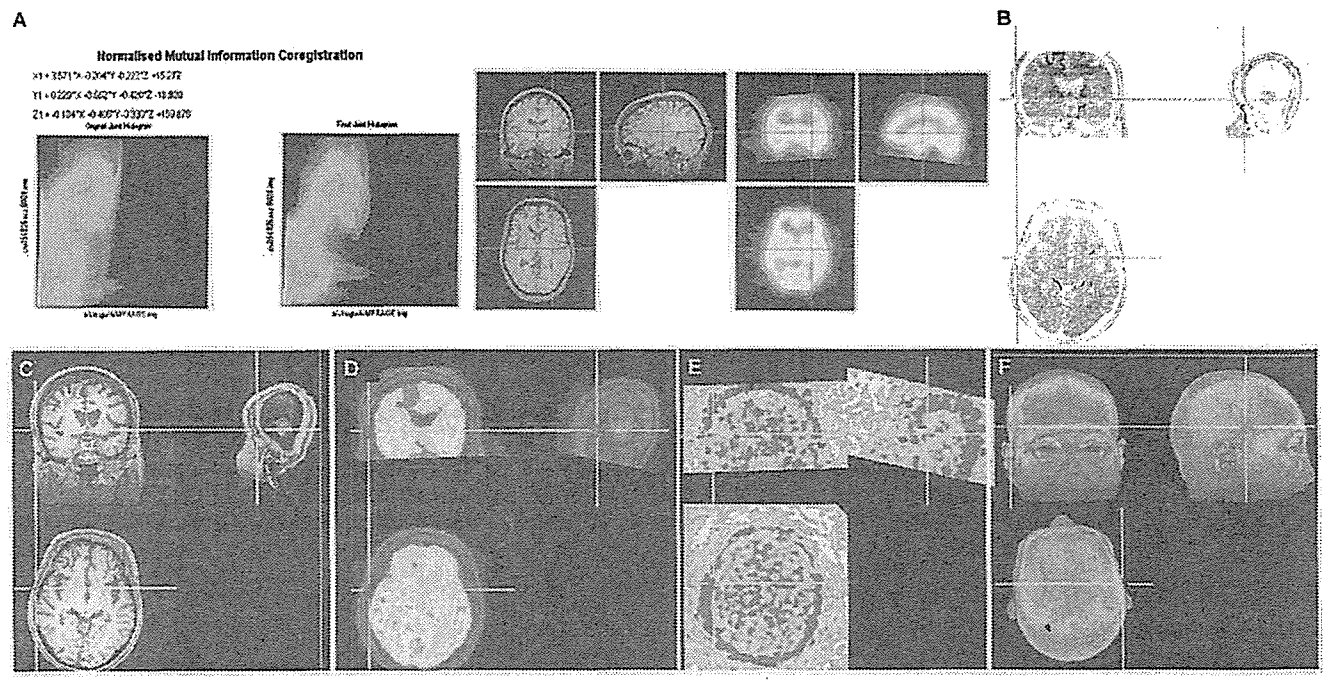


FIGURE 1. A, *MRA and rCBF data sets were registered with the MPRAGE data set by means of the coregistration function of the SPM2 software to render the registered data set available with the anatomic information of MPRAGE. By using MRIcro software and adjusting the slice and the region of interest* (cross bar), *we obtained coregistered three-dimensional images showing the arteries of the head* (B), *the anatomic structures of the brain* (C), *the distribution of the rCBF* (D), *the distribution of the regional oxygen extraction fraction* (E) *(only in cases with PET studies), and the surface of the scalp* (F).

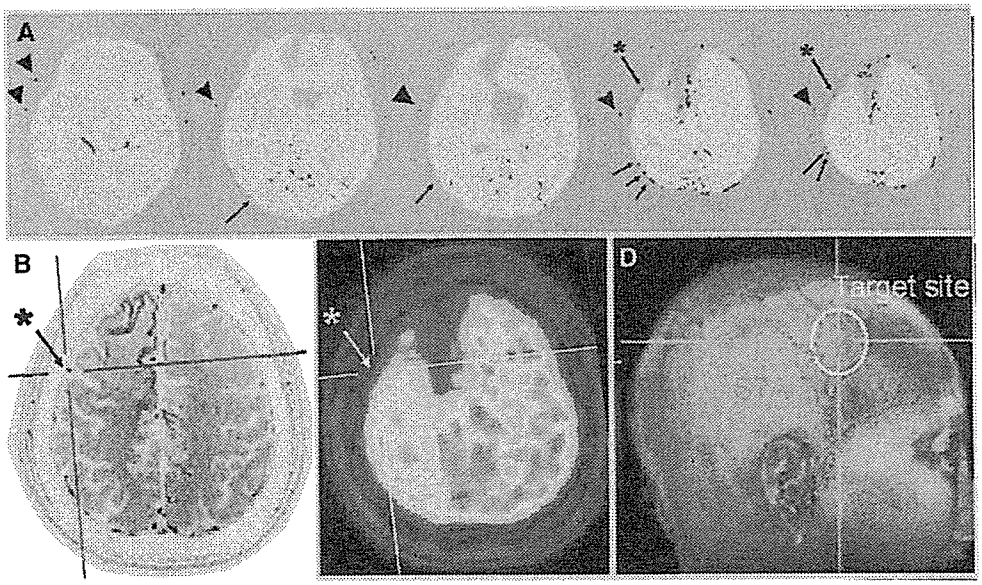


**FIGURE 2.** A–C, *fusion images between the MRA and rCBF data sets were obtained using the MRIcro software. Candidate recipient arteries could be found on the cortex of the right hemisphere* (arrowheads, *STA;* arrows, *candidate recipient arteries). As for the target* (asterisks *in* A–C), *we selected the cortical artery with the largest diameter from the candidates located on or near the cortex where the rCBF was markedly decreased.* D, *the location of the target in the coregistered scalp images was visible, which provided the site of the craniotomy.*

angle, 8 degrees; matrix, 256 × 240; field of view, 24 cm; 208 slices; slice thickness, 1 mm; no interslice gap; single averaging) and three-dimensional time-of-flight magnetic resonance angiography (MRA) (TR, 22 ms; TE, 3.84 ms; flip angle, 18 degrees; slice thickness, 0.64 mm; matrix, 512 × 208; acquisition time, 5 min 24 s; 192 slices) (5, 16). Quantitative regional cerebral blood flow (rCBF) was evaluated by iodine-123-labeled N-isopropyl-iodoamphetamine-single-photon emission computed tomography with a three-head rotating gamma camera (PRISM 3000; Shimazu Co., Ltd., Kyoto, Japan) or a $^{15}O_2$ gas steady-state positron emission computed tomography (PET) study with a PET scanner (Advance; General Electric, Milwaukee, WI) as reported previously (15, 19, 21). The MRA and rCBF data sets were registered with the MPRAGE data set through the coregistration function of the SPM2 software (Wellcome Department of Imaging Neuroscience, London, England) to create a registered data set with anatomic information of MPRAGE (*Fig. 1A*). Postoperative 3-Tesla magnetic resonance and single-photon emission computed tomographic studies were performed between 2 weeks and 1 month after the surgeries.

### Preoperative Targeting of the Recipient Artery

By adjusting the slice and the region of interest with free MRIcro software (http://www.mricro.com/) and using the coregistered data set of MPRAGE, MRA, and rCBF, it is possible to obtain coregistered three-dimensional images showing the arteries in the head (*Fig. 1B*), the anatomic structures of the brain (*Fig. 1C*), the distribution of the rCBF (*Fig. 1D*), the distribution of the regional oxygen extraction fraction (*Fig. 1E*) (only in cases with PET studies), and the surface of the scalp (*Fig. 1F*) (18). This software also enables the fusion of MRA and rCBF images (*Fig. 2A*). Some candidate arteries for the surgery can be found in these consecutive fusion images (*Fig. 2A*). From them, we selected as the target the artery with the largest diameter that was located on or near the cortex where rCBF was markedly decreased (*Fig. 2, B* and *C*). The location of the target in the coregistered scalp images could also be detected, which provided the site for the craniotomy (*Fig. 2D*). This approach enabled preoperative targeting of a recipient artery.

### Operative Procedures

On the day before surgery, a three-dimensional high-resolution computed tomographic scan of the whole brain was obtained with a 64-detector-row computed tomographic scanner (Aquilion; Toshiba Medical, Tokyo, Japan) to obtain the reference images. The rCBF, MRA, and three-dimensional computed tomographic data sets were applied to the neuronavigation system (Stealth Station; Medtronic, Sofamor Danek, Memphis, TN) and the fusion process was carried out with these images (6). With the patient under general anesthesia, we made the scalp incision after determining the location of the target on the scalp (*Fig. 3A*). The actual location of the target beneath the scalp was revealed through the navigation system, which displayed images of the cranium (*Fig. 3B*), MRA (*Fig. 3C*), and rCBF imaging (*Fig. 3D*), as well as a magnified image of the MRA (*Fig. 3E*). The location of the craniotomy and the design of the scalp incision were determined according to the location of the target and course of the STA (*Fig. 3, F* and *G*). After performing a small craniotomy (*Fig.3H*) and dural incision, we exposed the target at the center of the craniotomy (*Fig. 3I*). The STA was successfully anastomosed to the target (*Fig. 3J*).

## RESULTS

All surgeries were performed through a relatively small craniotomy. The patency of the bypass to the target and the postoperative improvement of rCBF was confirmed in all cases by coregistered images between MRA and rCBF imaging (*Table 1*).

## ILLUSTRATIVE CASES

### *Patient 3*

A 56-year-old woman with moyamoya-like disease underlying diabetes mellitus was admitted to our institution after a second cerebral

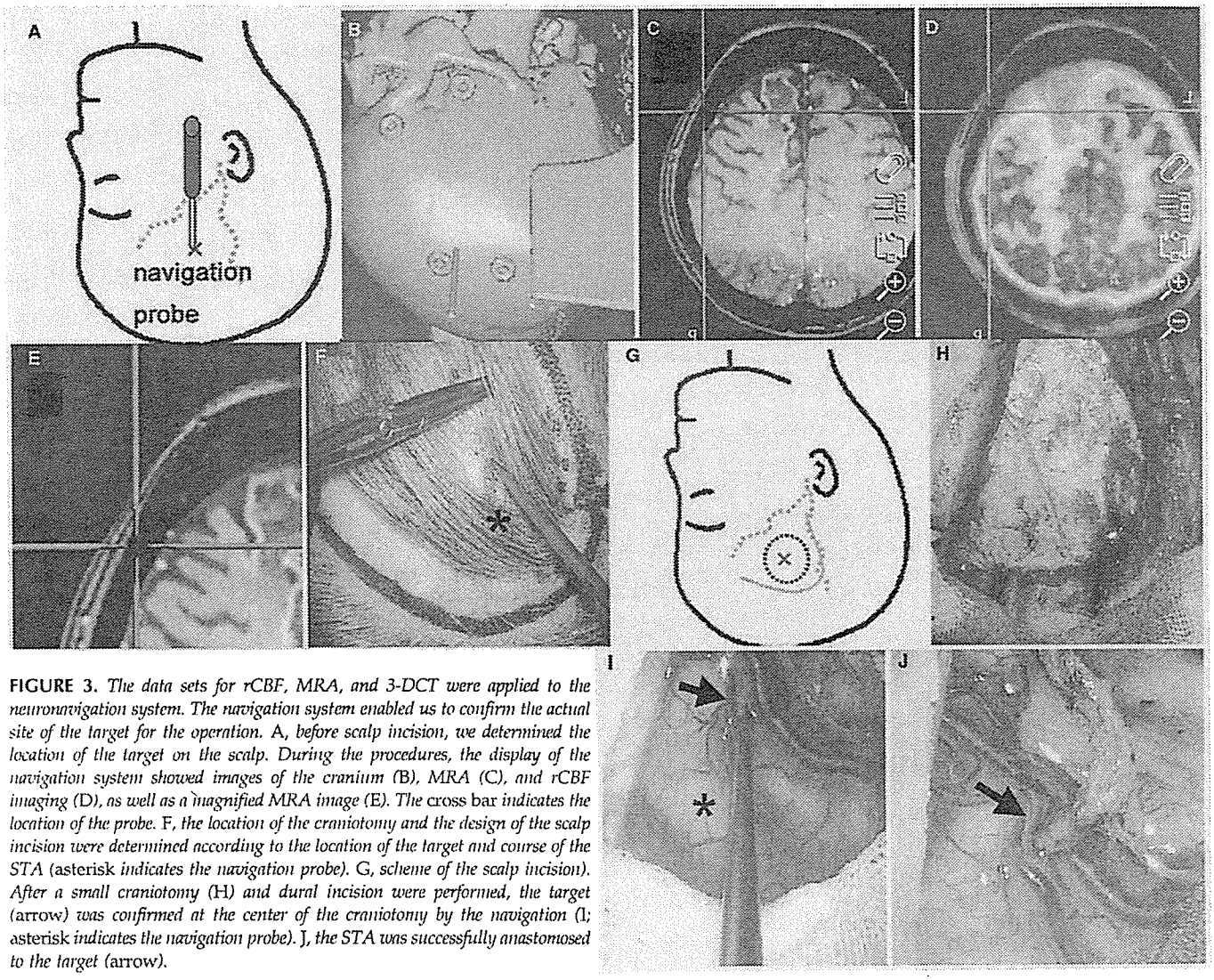


**FIGURE 3.** *The data sets for rCBF, MRA, and 3-DCT were applied to the neuronavigation system. The navigation system enabled us to confirm the actual site of the target for the operation.* A, *before scalp incision, we determined the location of the target on the scalp. During the procedures, the display of the navigation system showed images of the cranium* (B), *MRA* (C), *and rCBF imaging* (D), *as well as a magnified MRA image* (E). *The* cross bar *indicates the location of the probe.* F, *the location of the craniotomy and the design of the scalp incision were determined according to the location of the target and course of the STA* (asterisk *indicates the navigation probe).* G, *scheme of the scalp incision). After a small craniotomy* (H) *and dural incision were performed, the target* (arrow) *was confirmed at the center of the craniotomy by the navigation* (I; asterisk *indicates the navigation probe).* J, *the STA was successfully anastomosed to the target* (arrow).

infarction in the right frontal lobe (*Fig. 4A*). Before surgery, she presented with transient ischemic attacks of the left hemiparesis occurring several times a day. A preoperative single-photon emission computed tomographic study revealed a significant decrease in rCBF (*Fig. 4B*) and regional cerebrovascular reserve under acetazolamide challenging dominantly in the right frontal lobe. Cerebral angiography revealed a right MCA occlusion (*Fig. 4, C* and *D*) and stenosis at the terminal portion of the left ICA (*Fig. 4, E* and *F*). STA-MCA anastomosis on the right side was planned. Although few cortical branches of the right MCA could be visualized in the angiograms, our method enabled preoperative targeting of a recipient artery in the right frontal lobe (*Figs. 2* and *3*). Postoperative studies revealed the patency of the bypass to the target (*Fig. 4, G* and *H*) through improved rCBF in the right hemisphere (*Fig. 4I*). This patient's transient ischemic attacks disappeared after surgery.

### Patient 4

A 63-year-old woman with MMD presented with incomplete Gerstmann's syndrome caused by completed stroke. She underwent left STA-MCA anastomosis. Preoperative targeting of a recipient artery (*Fig. 5, A–C*) and bypass surgery were performed in the same manner as in Patient 3. We exposed the targeted recipient artery at the center of the craniotomy (*Fig. 5, E* and *F*) through a quarter-sized craniotomy. The STA was successfully anastomosed to the target (*Fig. 5G*).

## DISCUSSION

STA-MCA anastomosis was first reported by Yaşargil (22) in 1969. Although the international trial in 1985 (3) failed to prove this surgery's prophylactic effects against recurrent stroke (3), the Japanese extracranial-intracranial bypass trial (JET study) completed its evaluation of the validity of STA-MCA anastomosis in intracranial arterial occlusive disease in preventing hemodynamic stroke (15). Moreover, a carotid occlusion surgery study is ongoing in the United States.

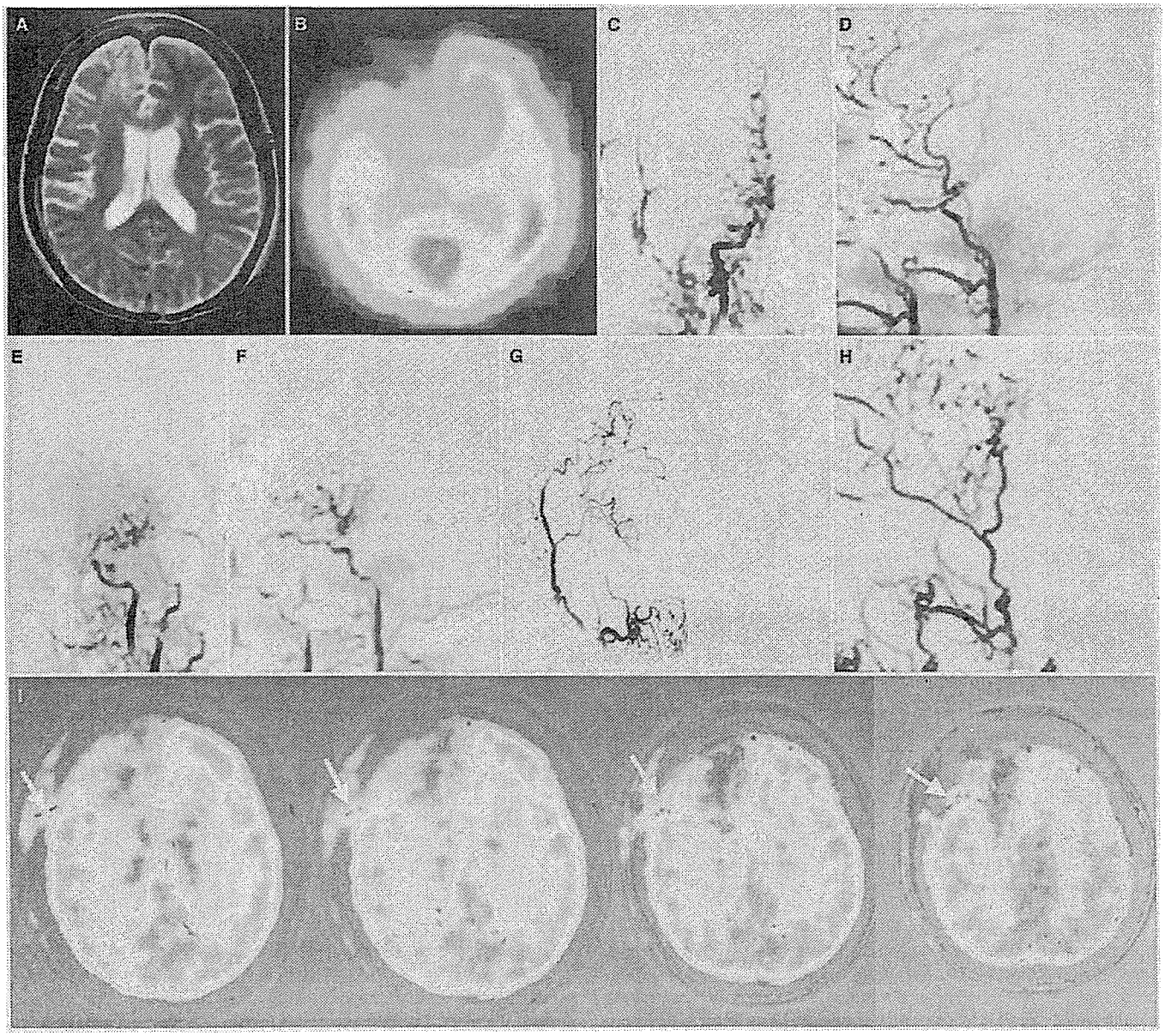


**FIGURE 4.** *Right STA-MCA anastomosis for a 56-year-old woman (Patient 3) with moyamoya-like disease. A, T2-weighted magnetic resonance imaging scan obtained on admission demonstrating cerebral infarction in the right frontal lobe. B, a preoperative single-photon emission computed tomographic study revealing significantly decreased rCBF, mainly in the right frontal lobe. C–F, cerebral angiography revealing right MCA (C and D) occlusion and stenosis at the terminal portion of the left ICA (E and F). Postoperative external angiograms in the anteroposterior (G) and lateral (H) views showing the patency of the bypass. I, postoperative fusion images between the MRA and rCBF showed the success of the bypass to the target (arrows) with improvement in rCBF in the right hemisphere.*

In Japan, STA-MCA anastomosis has especially been applied to the treatment of MMD (8, 13). Although direct bypass surgery, such as STA-MCA anastomosis, was reported to be more effective than indirect anastomosis in the treatment of MMD (2, 7, 10, 12, 18), indirect bypass methods, such as encephaloduroarteriosynangiosis, have often been preferred because of the technical difficulty of direct bypass (12). Moreover, in addition to the technical difficulty of the anastomotic procedure itself, finding recipient arteries with a suitable diameter for anastomosis is difficult during surgery for MMD (8, 9, 12). In our institution, STA-MCA anastomosis has been performed in all cases of MMD or moyamoya-like disease (13). Although the results of our surgery have been quite favorable, a relatively large craniotomy in the frontotemporal region is

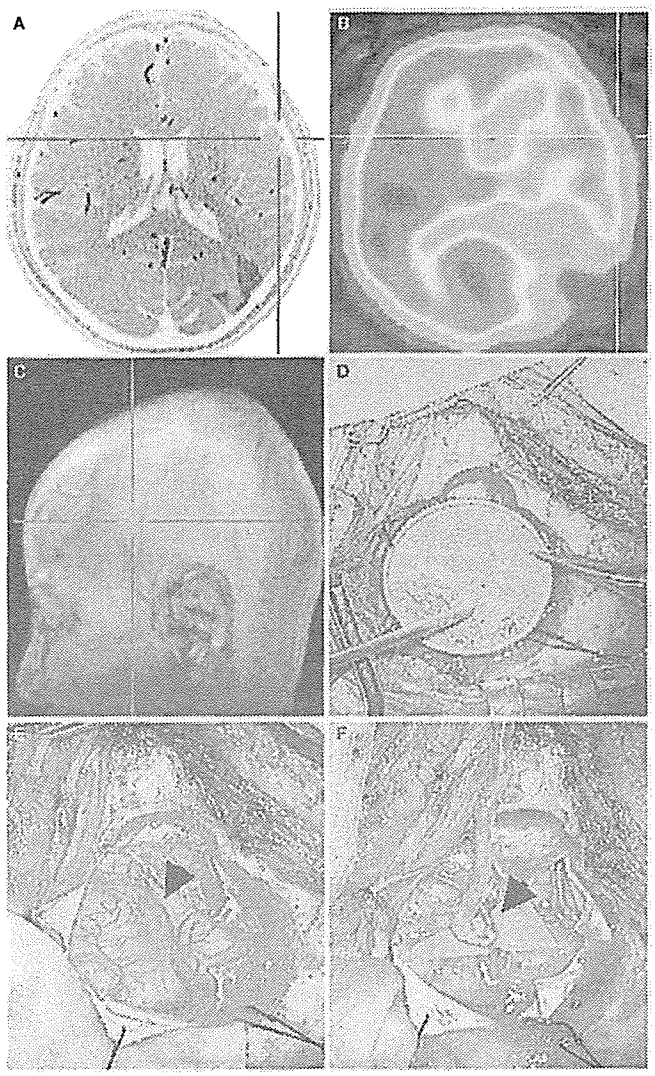


FIGURE 5. *Left STA-MCA anastomosis in a 63-year-old woman with MMD (Patient 4). Preoperative targeting of a recipient artery* (A, *MRA*; B, *rCBF*; C, *scalp imaging*) *and bypass surgery in the same manner as in Patient 3. A craniotomy the size of a quarter* (D) *was used to expose the targeted recipient artery at the center of the craniotomy* (E) *and enabled success bypass to the target* (F). *Target indicated by* arrowheads.

routinely required to reveal a proper recipient artery for the operation (8, 13).

One of the advantages of our method is the identification of the location of the recipient artery with pinpoint accuracy before scalp incision. Even in cases, such as those of MMD, in which preoperative angiograms demonstrate only a few candidates for recipient artery, an appropriate recipient artery can be exposed at the center of craniotomy with our method. Therefore, our method is considered effective in surgery for most cases of MMD.

A second advantage of our method is the use of a small craniotomy for STA-MCA anastomosis. In this study, bypass surgery could be performed through a small craniotomy, even in patients with MMD. However, in some MMD patients, especially pediatric patients, an indirect bypass, such as encephalomyo-synangiosis, should be combined with a direct bypass through a large craniotomy (13). Thus, we do not recommend surgery through a small craniotomy with our method for all cases of MMD. Bypass surgery through a small craniotomy is also indicated for cases in which surgery must be performed quickly. Our method might be useful in STA-MCA anastomotis for patients with systemic disease, such as a heart dysfunction.

In this study, we performed three-dimensional time-of-flight MRA with a 3-Tesla unit to target a recipient artery. MRA principally describes only arteries because it selectively detects and captures signals moving at high velocity. As reported previously, three-dimensional time-of-flight MRA with a 3-Tesla unit can well describe small arteries with a diameter less than 1 mm, such as moyamoya vessels (5). In this study, MRA also clearly described arteries having a diameter of approximately 1 mm on the brain surface or within the scalp. Although brain shift has been raised as a significant issue with image-guided neuronavigation surgery (6), it was not a significant problem with our method because use of the navigation system was concluded before scalp incision.

A third advantage of our method is the targeting of a recipient artery with reference to an rCBF map to achieve selective revascularization of the region with decreased rCBF. In this report, among the arteries situated on or near the cortex where rCBF was significantly decreased, we selected the cortical artery with the largest diameter as the target. However, whether or not our approach for determining the target is the best for preventing recurrent stroke remains controversial, and this might be one of the greatest problems with our method. It is possible that the best target is an artery with the largest diameter located other than in the region presenting decreased rCBF. An artery in the cortex in the region with the most significant decrease in rCVR (23) or with highest increase in rOEF in the PET study (20) might be a more suitable target. This issue should be investigated further.

## CONCLUSION

The "target bypass" method can provide preoperative identification of the location of a proper recipient artery in STA-MCA anastomosis. This method might be effective for patients with MMD or those requiring surgery through a small craniotomy. Methods of determining the optimal target recipient artery should be further investigated.

## REFERENCES

1. Coenen VA, Krings T, Weidemann J, Hans FJ, Reinacher P, Gilsbach JM, Rohde V: Sequential visualization of brain and fiber tract deformation during intracranial surgery with three-dimensional ultrasound: An approach to evaluate the effect of brain shift. **Neurosurgery** 56 [Suppl 1]:133–141, 2005.
2. Cahan LD: Failure of encephalo-duro-arterio-synangiosis procedure in moyamoya disease. **Pediatr Neurosci** 12:58–62, 1985.

3. EC/IC Bypass Study Group: Failure of extracranial-intracranial arterial bypass to reduce the risk of ischemic stroke. Results of an international randomized trial. **N Engl J Med** 313:1191–1200, 1985.
4. Fukui M: Guidelines of the diagnosis and treatment of spontaneous occlusion of the circle of Willis (moyamoya disease). **Clin Neurol Neurosurg** 99 [Suppl 2]:S238–S240, 1997.
5. Fushimi Y, Miki Y, Kikuta K, Kanagaki M, Yamamoto A, Nozaki K, Hashimoto N, Hanakawa T, Fukuyama H, Togashi K: Comparison of 3.0- and 1.5-T three-dimensional time-of-flight MR angiography in moyamoya disease: A preliminary study. **Radiology** 239:232–237, 2006.
6. Gralla J, Guzman R, Brekenfeld C, Remonda L, Kiefer C: High-resolution three-dimensional T2-weighted sequence for neuronavigation: A new setup and clinical trial. **J Neurosurg** 102:658–663, 2005.
7. Houkin K, Kuroda S, Ishikawa T, Abe H: Neovascularization (angiogenesis) after revascularization in moyamoya disease. Which technique is most useful for moyamoya disease? **Acta Neurochir (Wien)** 142:269–276, 2000.
8. Karasawa J, Kikuchi H, Furuse S, Kawamura J, Sakaki T: Treatment of moyamoya disease with STA-MCA anastomosis. **J Neurosurg** 49:679–688, 1978.
9. Kawashima M, Rhoton AL Jr, Tanriover N, Ulm AJ, Yasuda A, Fujii K: Microsurgical anatomy of cerebral revascularization. Part I: Anterior circulation. **J Neurosurg** 102:116–131, 2005.
10. Matsushima T, Inoue T, Suzuki SO, Fujii K, Fukui M, Hasuo K: Surgical treatment of moyamoya disease in pediatric patients—Comparison between the results of indirect and direct revascularization procedures. **Neurosurgery** 31:401–405, 1992.
11. Matsushima Y, Inaba Y: Moyamoya disease in children and its surgical treatment. Introduction of a new surgical procedure and its follow-up angiograms. **Childs Brain** 11:155–170, 1984.
12. Miyamoto S, Kikuchi H, Karasawa J, Nagata I, Yamazoe N, Akiyama Y: Pitfalls in the surgical treatment of moyamoya disease. Operative techniques for refractory cases. **J Neurosurg** 68:537–543, 1988.
13. Miyamoto S, Nagata I, Hashimoto N, Kikuchi H: Direct anastomotic bypass for cerebrovascular moyamoya disease. **Neurol Med Chir (Tokyo)** 8 [Suppl]:294–296, 1998.
14. Mizumura S, Nakagawara J, Takahashi M, Kumita S, Cho K, Nakajo H, Toba M, Kumazaki T: Three-dimensional display in staging hemodynamic brain ischemia for JET study: Objective evaluation using SEE analysis and 3D-SSP display. **Ann Nucl Med** 18:13–21, 2004.
15. Nishizawa S, Yonekura Y, Tanaka F, Fujita T, Tsuchimochi S, Ishizu K, Okazawa H, Tamaki N, Konishi J: Evaluation of a double-injection method for sequential measurement of cerebral blood flow with iodine-123-iodoamphetamine. **J Nucl Med** 36:1339–1345, 1995.
16. Okada T, Mikuni N, Miki Y, Kikuta K, Urayama S, Hanakawa T, Fushimi Y, Yamamoto A, Kanagaki M, Fukuyama H, Hashimoto N, Togashi K: Integration of diffusion tensor tractography of the corticospinal tract using 3T with intraoperative white matter stimulation mapping: Preliminary result to validate corticospinal tract localization. **Radiology** (in press).
17. Roden C, Brett M: Stereotaxic display of brain lesions. **Behav Neurol** 12: 191–200, 2000.
18. Touho H, Karasawa J, Ohnishi H, Yamada K, Shibamoto K: Surgical reconstruction of failed indirect anastomosis in childhood moyamoya disease. **Neurosurgery** 32:935–940, 1993.
19. Ueno M, Nishizawa S, Toyoda H, Shimono T, Miyamoto S, Hashimoto N, Konishi J: Assessment of cerebral hemodynamics before and after revascularization in patients with occlusive cerebrovascular disease by means of quantitative IMP-SPECT with double-injection protocol. **Ann Nucl Med** 15:209–15, 2001.
20. Yamauchi H, Fukuyama H, Nagahama Y: Significance of increased oxygen extraction fraction in five-year prognosis of major cerebral arterial occlusive disease. **J Nucl Med** 40:1992–1998, 1999.
21. Yamauchi H, Fukuyama H, Nagahama Y, Nishizawa S, Konishi J: Uncoupling of oxygen and glucose metabolism in patients with crossed cerebella diaschisis. **Stroke** 30:1424–1428, 1999.
22. Yaşargil MG: Anastomosis between the superficial temporal artery and a branch of the middle cerebral artery, in Yaşargil MG (ed): *Microsurgery Applied to Neurosurgery*. Stuttgart, George Thieme Verlag, 1969, pp 105–115.
23. Yokota C, Hasegawa Y, Minematsu K: Effect of acetazolamide reactivity on long-term outcome in patients with major cerebral artery occlusive diseases. **Stroke** 29:640–644, 1998.

## COMMENTS

In this article, the authors have described the preoperative targeting of the superficial temporal artery-to-middle cerebral artery (STA-MCA) bypass using preoperative study of cerebral blood flow and fusion of this information with other imaging data. They used it successfully in patients with moyamoya syndrome. This seems to be a good strategy in the short term. Over the long term, however, the bypass donor artery is expected to enlarge and supply a much larger vascular territory through collateral circulation, and the technique may be less important.

An important issue to be considered is that the ischemic territory of the brain undergoes additional ischemia during the bypass procedure, and may be more susceptible to a stroke. The question would be whether or not it is better to place the bypass in the penumbra zone of the ischemic territory because, in time, the donor vessel would be expected to also supply the densely ischemic region.

In the United States, vascular bypasses for ischemia (not aneurysms or basal tumors) are routinely performed only for moyamoya syndrome. For patients with atherosclerotic occlusive disease, such bypasses are being reimbursed by Medicare only as part of the Carotid Occlusion Surgery Study trial, even though there are patients who have failed maximal medical therapy and, for one reason or another, do not qualify for the Carotid Occlusion Surgery Study trial. This is not true in Japan, where STA-MCA bypasses are still being performed in large numbers for cerebral ischemia secondary to atherosclerotic vascular occlusion.

**Laligam N. Sekhar**
*Seattle, Washington*

Kikuta et al. apply multiple imaging modalities (magnetic resonance angiography [MRA] and three-dimensional [3-D] computed tomographic scanning) to target the donor STA and an appropriate sized MCA recipient branch in moyamoya disease or moyamoya-like disease. In addition, the authors use various cerebral blood flow studies (single-photon emission computed tomography and positron emission tomography [PET]) to determine regions of hypoperfusion for targeting in these patients. This technique was successful in six (STA-MCA) bypass operations. The authors admit that this is a technical report and do not provide evidence that this will help patient outcome. However, this article is important because it may reduce the number of indirect bypass procedures that are used because of inadequate recipient arteries, and it allows for a smaller craniotomy, which may reduce operative time and, possibly, morbidity. The authors appropriately state that it remains unclear whether or not targeting a recipient artery in areas of hypoperfusion is beneficial to patient outcome. One limitation of this study is that it only involves six study subjects. However, the technique is extremely novel and seems feasible. Further experience with this method, combined with assessment of clinical outcomes, will determine its efficacy.

**Gary K. Steinberg**
**Michael E.B. Kelly**
*Stanford, California*

The au ıave developed a technique using a unique software applic y which a revascularization procedure can be targeted very specifically to a certain area of cerebral cortex that appears maxi-

mally threatened on physiological imaging. To accomplish this, 3 T magnetic resonance imaging scans, magnetization prepared rapid gradient echo-water excitation, 3-D time-of-flight, MRA, and color Doppler flow studies with either single-photon emission computed tomography or PET are acquired preoperatively. At surgery, the color Doppler flow and MRA images are coregistered with the 3-D high-resolution computed tomographic scan to perform intraoperative localization. As a result, very small craniotomies are possible to direct flow from an extracranial to intracranial bypass into a very specific area.

This is an interesting and intuitive application of current image fusion techniques. It enables the surgeon to target a specific recipient artery that is size matched to the donor STA. Potential difficulties in applying this technique include considerations of whether or not the STA maintains adequate diameter once you reach a peripheral target. In addition, one wonders if it might be more appropriate to target a larger recipient (with a larger donor) more proximally along the arterial tree to the area of maximal ischemia. Possibly, in using that mechanism, even more flow could be directed to the specific target region. Nevertheless, this is an interesting study that should stimulate all of us to be more creative as we approach patients with complicated ischemic state.

**H. Hunt Batjer**
*Chicago, Illinois*

The authors have described an innovative technique to preoperatively identify the recipient artery when performing STA-MCA anastomosis. Images of the angioarchitecture are obtained by MRA and fused with regional cerebral blood flow examinations obtained either by single-photon emission computed tomography or PET. The authors were able to coregister 3-D images of the arteries, the anatomic structures of the brain, and the distribution of the regional cerebral blood flow or regional oxygen extraction fraction (if PET studies were used). This allowed the authors to identify the recipient artery on the basis of diameter as well as region of decreased cerebral blood flow.

The primary advantages of this technique, as expressed by the authors, include the ability to use a very small craniotomy by preselecting the recipient artery and the ability to identify the region of decreased cerebral blood flow. Although the size of the craniotomy for an extracranial to intracranial bypass does not dictate the length of the operation to any great degree, there is some benefit of being able to preoperatively identify a recipient artery of adequate size. Whether or not a bypass performed in an area of greater decreased cerebral blood flow is advantageous remains to be proven. Patients with moyamoya disease or MCA occlusion may well redistribute the additional blood flow through the patent anastomosis to the regions of ischemia. Certainly, further work is indicated to determine the precise benefit of this technique. Notwithstanding these cautionary comments, the authors have demonstrated an elegant technique for identifying a suitable recipient vessel for extracranial to intracranial bypass in a highly reproducible manner.

**Daniel L. Barrow**
*Atlanta, Georgia*

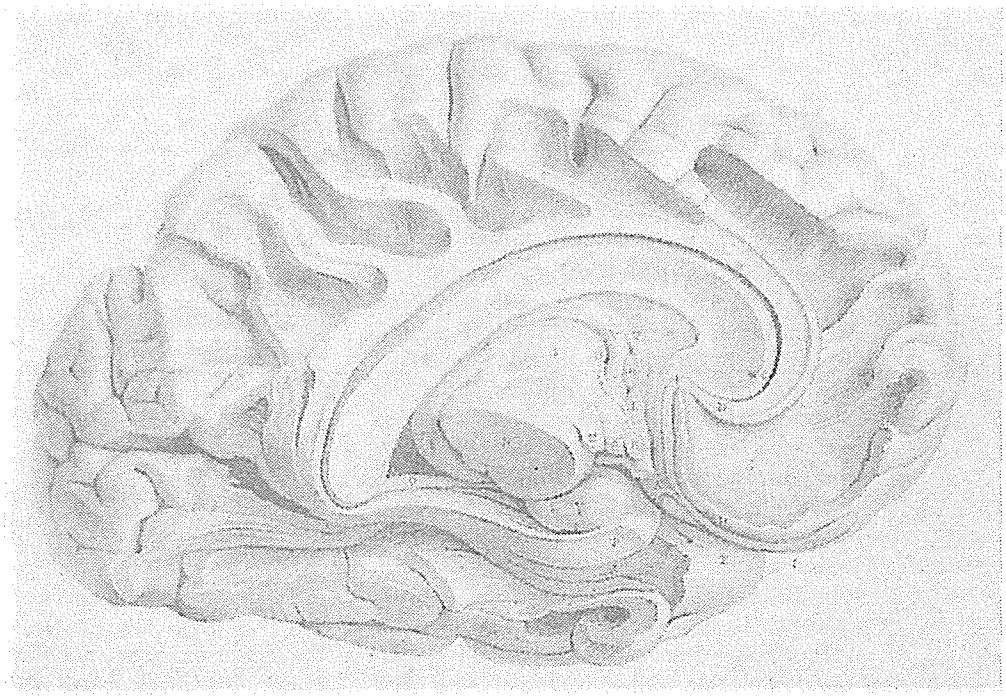

*Achille Louis Foville, 1799-1878,* ***Traité Complet de l'anatomie, de la Physiologie et de la Pathologie du Système Nerveux Cérébro-spinal.*** *Paris: Fortin, Masson, 1844 (Courtesy, Rare Book Room, Norris Medical Library, Keek School of Medicine, University of Southern California, Los Angeles, California.)*

**Tsuyoshi Ohta, M.D.**
Department of Neurosurgery,
Graduate School of Medicine,
Kyoto University,
Kyoto, Japan

**Ken-ichiro Kikuta, M.D., Ph.D.**
Department of Neurosurgery,
Graduate School of Medicine,
Kyoto University,
Kyoto, Japan

**Hirotoshi Imamura, M.D.**
Department of Neurosurgery,
Graduate School of Medicine,
Kyoto University,
Kyoto, Japan

**Yasushi Takagi, M.D., Ph.D.**
Department of Neurosurgery,
Graduate School of Medicine,
Kyoto University,
Kyoto, Japan

**Masaki Nishimura, M.D., Ph.D.**
Department of Neurosurgery,
Graduate School of Medicine,
Kyoto University,
Kyoto, Japan

**Yoshiki Arakawa, M.D., Ph.D.**
Department of Neurosurgery,
Graduate School of Medicine,
Kyoto University,
Kyoto, Japan

**Nobuo, Hashimoto, M.D., Ph.D.**
Department of Neurosurgery,
Graduate School of Medicine,
Kyoto University,
Kyoto, Japan

**Kazuhiko Nozaki, M.D., Ph.D.**
Department of Neurosurgery,
Graduate School of Medicine,
Kyoto University,
Kyoto, Japan

**Reprint requests:**
Ken-ichiro Kikuta, M.D., Ph.D.,
Department of Neurosurgery,
Graduate School of Medicine,
Kyoto University,
54 Kawaharacho, Shogoin,
Sakyo-ku, Kyoto 606-8507, Japan.
Email: kikuta@kuhp.kyoto-u.ac.jp

**Received**, October 24, 2005.
**Accepted**, May 10, 2006.

# ADMINISTRATION OF EX VIVO-EXPANDED BONE MARROW-DERIVED ENDOTHELIAL PROGENITOR CELLS ATTENUATES FOCAL CEREBRAL ISCHEMIA-REPERFUSION INJURY IN RATS

**OBJECTIVE:** This study aimed to examine early effects of ex vivo-expanded bone marrow-derived endothelial progenitor cells (EPCs) on focal cerebral ischemia-reperfusion injury.

**METHODS:** EPCs were obtained from mononuclear cells of autologous bone marrow of a rat. After culture on fibronectin-coated dishes for 10 to 14 days, $2.5 \times 10^5$ cells of EPCs were administered transarterially after 90 minute occlusion of the middle cerebral artery.

**RESULTS:** Administration of EPCs significantly reduced both the infarct volume and the scores of neurological deficits at 24 and 48 hours. EPCs administered 2 hours after insult did not reduce infarct volume, but attenuated neurological deficits at 24 hours. Administration of EPCs significantly reduced the number of myeloperoxidase-immunoreactive cells in the ischemic lesion at 24 hours and increased regional cortical blood flow at 48 hours. EPCs were observed in the ischemic hemisphere and around the endothelial layer of the pial arteries. Most of them expressed endothelial nitric oxide synthase.

**CONCLUSION:** Administration of ex vivo-expanded bone marrow-derived EPCs reduced infarct volume and neurological deficits in acute focal brain ischemia-reperfusion injury caused, at least in part, by attenuation of endothelial dysfunction.

**KEY WORDS:** Cerebral infarction, Endothelial dysfunction, Endothelial progenitor cells

*Neurosurgery 59:679-686, 2006* DOI: 10.1227/01.NEU.0000229058.08706.88 www.neurosurgery-online.com

Endothelial progenitor cells (EPCs) were first discovered in the leukocyte fraction of human peripheral blood that expressed CD34 on the cell surface (2). EPCs can be isolated from umbilical cord blood, peripheral blood, or bone marrow (BM) (3, 5, 19, 26). Mobilization of EPCs from BM to peripheral blood is enhanced in pathological conditions such as tissue ischemia, wound healing, and focal cerebral ischemia for promoting local angiogenesis (1, 2, 34, 37). Local injection of ex vivo-expanded EPCs can reduce hind limb ischemia and myocardial infarction (19, 20). Beneficial effects of EPCs on focal cerebral ischemia in the chronic stage were reported (37), but early effects have not been fully clarified. In this study, we focused on the early effects of transarterial administration of ex vivo-expanded BM-derived EPCs on focal cerebral ischemia-reperfusion injury.

## METHODS

### Animals

All procedures were performed in accordance with the guidelines of the Animal Research Committee of Kyoto University Graduate School of Medicine. Male Sprague-Dawley rats weighing 280 to 300 g (age, 8–10 wk) were obtained from Shimizu Laboratory Supplies Co., Ltd. (Kyoto, Japan).

### Preparation of BM-derived EPCs

EPCs were obtained from autologous BM of rats (22). BM was aspirated from the shaft of the femur under general anesthesia with halothane. Mononuclear cell fractions were isolated by centrifugation with Ficoll-Paque density gradient (Pharmacia, Uppsala, Sweden) (19, 26). Cells were resuspended in endothelial

cell (EC) basal medium-2 (Cambrex Corp., East Rutherford, NJ) plus microvascular endothelial cell medium-2 SingleQuots containing 5% fetal bovine serum, human vascular endothelial growth factor (VEGF)-1, human fibroblast growth factor-2, human epidermal growth factor, insulin-like growth factor (IGF)-1, and ascorbic acid and cultured on a fibronectin-coated dish (Biocoat, Fort Washington, PA) at 37°C under 5% carbon dioxide. On Day 4, nonadherent cells were removed, and adherent cells were cultured and maintained 6 to 10 more days.

### Cellular Staining

On Day 10, cultured cells were incubated with 1,1'-dioctadecyl-3,3,3',3'-tetramethylindocarbocyanine-labeled acetylated low-density lipoprotein (acLDL) (1:200; Molecular Probes, Eugene, OR) at 37°C for 4 hours and fixed with 4% phosphate-buffered paraformaldehyde (PBPA) for 10 minutes. Later, they were reacted with fluorescein isothiocyanate-conjugated *Bandeiraea simplicifolia* isolectin B4 (Sigma-Aldrich, St. Louis, MO) or with mouse monoclonal antibodies against von Willebrand Factor (vWF) (DAKO, Glostrup, Denmark) at 37°C for 4 hours (35).

### Immunoblotting

Immunoblotting with rabbit polyclonal antibodies against Flk-1 (NeoMarkers, Fremont, CA), Tie-2 (Sigma-Aldrich), goat polyclonal antibody against intracellular adhesion molecule (ICAM)-1(Sigma-Aldrich), mouse monoclonal antibodies against vWF (DAKO), or α-tubulin (Sigma-Aldrich) was performed on the cells on Day 10, and with human microvascular ECs (Cambrex) and human aortic smooth muscle cells (Cambrex), as previously reported (18).

### Transient Middle Cerebral Artery Occlusion of Rats and Transarterial Administration of EPCs

Methods for the preparation of a rat middle cerebral artery (MCA) occlusion model were described in our previous reports (4, 13, 14, 27, 30, 31, 32, 33). In the preliminary experiments, physiological parameters, including blood pressure and blood gas data, had been stabilized in the model to make the infarct volume stable and reproductive (4). Some modifications were added to a thread for arterial occlusion (23, 24). The thread consisted of a nylon monofilament and a polyethylene tube. Thirty-eight millimeters of 3–0 nylon monofilament was passed through a 15-mm polyethylene tube (inner diameter, 0.28 mm; outer diameter, 0.61 mm) (Natume, Tokyo, Japan). Both tails of the monofilament and the tube were fixed to each other with silicone (Heraeus Kulzer, Hanau, Germany). Thus, the tip of the thread consisted of a bare nylon monofilament (*Fig. 1G*). After surgical exposure and temporary occlusion of the common carotid artery and the internal carotid artery (ICA), the tip of the thread was navigated into the ICA through the external carotid artery (length, 19 mm). When the tip of the thread reached the top of the ICA, the tube was also introduced into the ICA proximal to the pterygopalatine artery (*Fig. 1G*). After 90-minute occlusion, only the nylon filament was withdrawn, and the tube remained within the ICA. Autologous EPCs on Day 10 of $2.5 \times 10^5$ suspended in 0.3 ml phosphate-buffered saline (PBS (-)) were injected into the ICA through the tube in 60 seconds. In the delayed group, EPCs were injected 2 hours after the reperfusion. The filament was completely withdrawn, and the stump of the external carotid artery was clipped for 2 hours without heparin. After that, only the tube was introduced into the ICA. After discontinuation of halothane, the rats recovered spontaneously. In the control rats, 0.3 ml PBS (-) or A10 (embryonic thoracic aorta, smooth muscle, DB1X

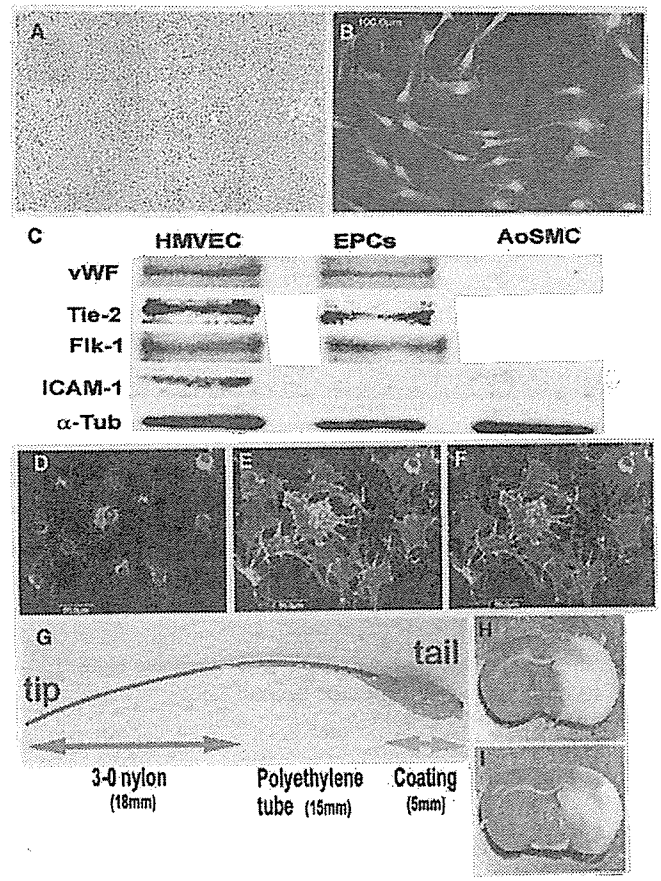


**FIGURE 1.** *Molecular characterization of EPCs and rat MCA occlusion model. Cells cultured for 10 days showed a typical cobblestone appearance (A) and expressed vWF (B). C, immunoblottings demonstrating vWF, Tie-2, Flk-1, and α-tubulin expression, but not ICAM-1. They incorporated 1,1'-dioctadecyl-3,3,3',3'-tetramethylindocarbocyanine-acLDL (D) and bound to fluorescein isothiocyanate-labeled lectin (E) and (F), merged.* Scale bars = *100 μm (B) and 50 μm (D–F). G, the thread for MCA occlusion was provided as a 38-mm 3–0 nylon monofilament passing through a 15-mm polyethylene tube (inner diameter, 0.28 mm; outer diameter, 0.61 mm) with its tail fixed to itself by silicone. The infarct lesion was defined as sparing site from 2,3,5-triphenyltetrazolium chloride staining. Representative photographs of lesion at 48 hours in control (H) and EPC (I) groups.*

rat) (Dainippon Pharmaceutical Co., Ltd., Osaka, Japan) was injected. During the entire procedure, the rectal temperature was kept between 36.5 and 37.0°C with a heating pad.

### Evaluation of Infarct Volume

Rats were deeply anesthetized with diethyl ether for 3 minutes at 24 or 48 hours. After decapitation, brains were quickly extracted, and coronal sections (thickness, 2 mm) were immersed in a 2% solution of 2,3,5-triphenyltetrazolium chloride (Sigma-Aldrich) in PBS (-) at 37°C for 30 minutes (28). They were digitally photographed, and the infarct volume was calculated using SCION imager (Scion Corp., Frederick, MD) (10). Infarct volume was expressed as the ratio of it to the volume of contralateral hemisphere in the same individual.

### Evaluation of Neurological Deficits

Motor function was evaluated at 24 or 48 hours with a walking trial on the rotating spindle of a Rota rod (Muromachi, Tokyo, Japan) (23). Rats were preconditioned to walk on the spindle at a constant speed of 2, 4, 6, and 8 revolutions per minute (rpm) until they were able to stay on it for 120 seconds. Thereafter, the rotating speed was set to increase to 40 rpm in 300 seconds, and the rpm at the time of falling was defined as the function score (12).

### Immunohistochemical Analysis of In Vivo Distribution of EPCs

Adenoviral vector for expression of green fluorescent protein (GFP, $4 \times 10^7$ PFU/ml, 2 multiplicity of infection) was transfected to EPCs on Day 8 (11) and administered to MCA occlusion or sham-operated rats 2 days after transfection. Extensive expression of GFP on EPCs between 24 to 72 hours later was confirmed in vitro (data not shown). Rats were perfused with PBS (-) and 4% PBPA under deep anesthesia at 24 and 48 hours and fixed with 4% PBPA for 24 hours and 0.5 mol/L sucrose for another 24 hours. Frozen coronal sections (thickness, 10 $\mu$m) from the center of the ischemic lesion at the level of the anterior commissure (interaural, 8.2 mm; bregma, 0.8 mm) were embedded in optimal cutting temperature compound (Sakura Finetechnical, Tokyo, Japan) and stained with mouse monoclonal antibodies against vWF (DAKO) or $\alpha$-smooth muscle actin (NeoMarkers). The relationships between EPCs and ICAM-1, VEGF, eNOS, and IGF-1 were examined in the paraffin-embedded 10-$\mu$m thick sections. After deparaffinization (xylen, 10 min; absolute alcohol, 10 min; 95% alcohol, 3 min; 70% alcohol, 3 min), they were stained with rabbit polyclonal and mouse monoclonal antibodies against GFP (Molecular Probes) and mouse monoclonal antibodies against ICAM-1 (Santa Cruz Biotechnology, Inc., Santa Cruz, CA), rabbit polyclonal antibodies against VEGF and eNOS (Lab Vision, Fremont, CA) ,and mouse monoclonal antibody against IGF-1 (Upstate, Charlottesville, VA). Then, they were reacted with goat antimouse monoclonal or rabbit polyclonal antibodies conjugating Alexa Fluor Dye (Molecular Probes) of each spectrum 488, 546, and 647. The confocal laser scanning microscope (Fluoview, FV300, Olympus, Japan) was used in this study.

### Measurement of Regional Cerebral Cortical Blood Flow

Regional cerebral cortical blood flow (rCoBF) at the same point of the brain surface was measured as previously reported, with modification (7). The dural surface in the right parietal cortex located at 2 mm lateral and 1 mm caudal to bregma (*Fig. 3A*) was surgically exposed under halothane, which was considered MCA territory around the ischemic core (24). A laser Doppler flowmeter probe (Flo-C1, Omegawave, Tokyo, Japan) was placed and fixed tightly with resin. On that day, transient MCA occlusion and EPC administration were performed. rCoBF was measured sequentially just before insult and at 24 and 48 hours under halothane (8, 33). The

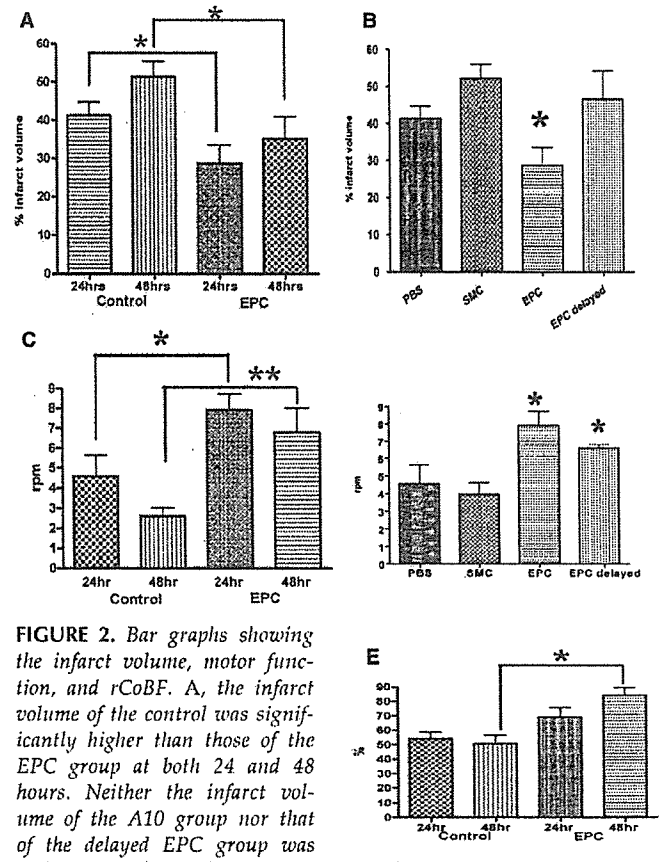


**FIGURE 2.** *Bar graphs showing the infarct volume, motor function, and rCoBF.* A, *the infarct volume of the control was significantly higher than those of the EPC group at both 24 and 48 hours. Neither the infarct volume of the A10 group nor that of the delayed EPC group was different from that of the PBS group 24 hours.* B, *only the early EPC group showed significant decrement.* C, *the motor function scores of the EPC group were significantly higher than the control both at 24 and 48 hours.* D, *both the early and delayed EPC groups showed significant improvement at 24 hours after ischemia in comparison with the A10 and PBS groups.* E, *rCoBF was significantly higher in the EPC group than in the control at 48 hours.* Single asterisk, $P < 0.05$; double asterisk, $P < 0.01$.